

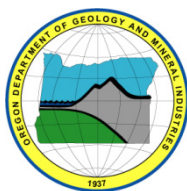
State of Oregon
Department of Geology and Mineral Industries
Vicki S. McConnell, State Geologist

Open-File Report O-12-01

**PRELIMINARY GEOLOGIC MAP OF THE MOUNT MCLOUGHLIN 7.5' QUADRANGLE,
JACKSON AND KLAMATH COUNTIES, OREGON**

By

Stanley A. Mertzman¹, Richard W. Hazlett², Stephen G. Weaver³, Isaac P. Weaver⁴, Jill M. Baum⁵,
Heidi M. Cruz⁶, Martha S. Gilmore⁴, Travis J. McElfresh⁷, Jonathon L. Nauert⁵,
Kirsten E. Nicolaysen⁸, James T. Rowe⁵, Andrew Tittler⁹, and Wayne R. Wright¹⁰



2012

¹Franklin and Marshall College, Department of Earth and Environment, Box 3003, Lancaster, Pennsylvania 17604

²Pomona College, Geology Department, 185 East 6th Street, Claremont, California 91711

³Colorado College, Department of Geology, 14 East Cache La Poudre, Colorado Springs, Colorado 80903

⁴Formerly at Franklin and Marshall College, Department of Earth and Environment, Box 3003, Lancaster, Pennsylvania 17604

⁵Formerly at Carleton College, Department of Geology, Mudd Hall, Northfield, Minnesota 55057

⁶Formerly at Amherst College, Department of Geology, 11 Barrett Hill Road, Amherst, Massachusetts 01002-5000

⁷Formerly at Whitman College, Department of Geology, Walla Walla, Washington 99362

⁸Formerly at Colorado College, Department of Geology, 14 East Cache La Poudre, Colorado Springs, Colorado 80903

⁹Formerly at Williams College, Geosciences Department, Clark Hall, 947 Main Street, Williamstown, Massachusetts 01267

¹⁰Formerly at Beloit College, Department of Geology, Beloit, Wisconsin 53511

NOTICE

This paper is being published as received from the author(s). No warranty, expressed or implied, is made regarding the accuracy or utility of the information described and/or contained herein, nor shall the act of distribution constitute any such warranty. This disclaimer applies both to individual use of the data and aggregate use with other data. The Oregon Department of Geology and Mineral Industries shall not be held liable for improper or incorrect use of this information.

Oregon Department of Geology and Mineral Industries Open-File Report O-12-01
Published in conformance with ORS 516.030

For copies of this publication or other information about Oregon's geology and natural resources, contact:

Nature of the Northwest Information Center
800 NE Oregon Street, Suite 965
Portland, Oregon 97232
(971) 673-2331
<http://www.naturenw.org>

For additional information:
Administrative Offices
800 NE Oregon Street, Suite 965
Portland, OR 97232
Telephone (971) 673-1555
Fax (971) 673-1562
<http://www.oregongeology.org>
<http://egov.oregon.gov/DOGAMI/>

Introduction

Mount McLoughlin, formerly known as Mount Pitt, is the most noteworthy topographic feature of the Mount McLoughlin 7.5' quadrangle. A master's thesis from the University of Oregon (Maynard, 1974) is the most recent attempt at understanding the geology of the Mount McLoughlin region. Mount McLoughlin easily forms the highest elevation in the quadrangle, 9,495 feet (2,894 m), while the lowest elevation is at the point where the North Fork of the Little Butte Creek exits the quadrangle in its southwest corner at an elevation $> 4,160$ and $< 4,200$ feet. Figure 1 provides the detailed geographic context for the Mount McLoughlin quadrangle and the immediately surrounding area. Figures 2A through 2D provide views of Mount McLoughlin, one of the High Cascade volcanoes, from each cardinal direction.

Mount McLoughlin is a composite volcano, or stratovolcano, much like a multilayer cake in which the sloping sides of the edifice are made up of layers of lava flows and pyroclastic material (see Figure 3) that vary in thickness (McBirney, 2007). A few miles to the south is Brown Mountain (see Figure 1 for its exact location and Figure 4 for a picture of the mountain), also a composite volcano, which is similar in geologic age to Mount McLoughlin. Figure 5 is a picture of both Mount McLoughlin and Brown Mountain that can be used as a basis for gross comparisons between the two volcanoes. The picture was taken from the south along the Old Baldy-Brush Mountain ridge looking to the north. For those readers who have traveled Oregon state highway 140 between Medford and Klamath Falls, the road goes between the two mountains, crossing the axis of the High Cascades at a pass 5,100 feet in elevation that separates the Klamath River drainage basin to the east from the Rogue River drainage basin to the west.

At first blush the slopes of Mount McLoughlin are clearly steeper than those formed on Brown Mountain. Viscosity is an important physical parameter controlling the slope angle in many volcanic landforms (Grotzinger and Jordan, 2010). The silica content of magma is the most important factor affecting viscosity: the higher the silica content, the greater the viscosity; therefore steeper slopes will result. With this in mind, examining Figure 5 would lead one to conclude that lower silica lavas dominate Brown Mountain whereas higher silica lavas, all other variables being equal, characterize Mount McLoughlin. Studying the chemical data contained in Table 1 clearly indicates a large majority of Mount McLoughlin cone-forming lavas and pyroclastics have silica contents in the 54 to 55 wt% SiO_2 range, while at Brown Mountain most silica values fall between 58 and 60 wt% SiO_2 . The chemical data are at odds with the suggestion that the silica content is the chief factor controlling viscosity and hence the slope angle of these two composite volcanoes. What other factors affect viscosity? Winter (2010) reported that temperature, volatile content, and phenocryst content also exert some control over viscosity in addition to chemical composition. Both temperature and volatile content vary inversely with viscosity; that is, as temperature and volatile content increase, viscosity decreases. Whereas plagioclase feldspar and pyroxene are the two dominant mineral constituents at both volcanoes, Mount McLoughlin rock samples normally contain several percent olivine, which is very rarely identified as a trace constituent of Brown Mountain lavas. The presence of olivine may thus indicate that Mount McLoughlin lavas were extruded at slightly higher magmatic temperatures than those of Brown Mountain. Mineral assemblages at both volcanoes are totally anhydrous indicating that volatile concentrations were relatively low to moderate in both magma-plumbing systems.

When it comes to phenocryst mineral content, however, there is a substantial difference between the volcanic rocks extruded from the two volcanoes. In Figure 6 a typical Mount McLoughlin pyroclast specimen is on the left and a typical lava specimen is on the right. The high phenocryst content, ranging between 25 and 40 percent with the modal amount of plagioclase feldspar > pyroxene (both clinopyroxene and orthopyroxene are present) > olivine (only 1 to 3 percent), is a ubiquitous characteristic of the cone-forming Mount McLoughlin samples. It is also important to note the dark spots that are present in virtually every Mount McLoughlin hand sample. These "spots" are glomeroporphyritic clumps or clots of early crystallizing minerals that are dominated by clinopyroxene and orthopyroxene (hence why the spots are dark in color) with lesser amounts of olivine and plagioclase that range in size from approximately 2 or 3 mm to 1 cm in diameter. Therefore, Mount McLoughlin lavas have two distinguishing petrographic characteristics: they are moderately to highly porphyritic and are invariably "spotted." The high phenocryst mineral content would noticeably increase the viscosity of the Mount McLoughlin lavas. The comparison with Brown Mountain extrusive material is stark (see Figure 7). Whereas the Mount McLoughlin lavas come with a highly visible mineral content, Brown Mountain does not. Brown Mountain lavas are noticeably aphyric; that is, they lack observable phenocrysts, even microphenocrysts. Except in very rare instances, all the mineral grains are less than 1 mm in diameter in Brown Mountain lavas.

In regard to parameters that affect viscosity (chemical composition, temperature, volatile content, phenocryst content), in this particular comparison of circumstantial physical evidence between Brown Mountain and Mount McLoughlin, the great disparity in phenocryst mineral content is an important factor in determining the external shapes of the two volcanoes seen in Figure 5. All composite volcanoes are not created equal; that is, the proportion of lava flows to pyroclastics can vary within fairly broad limits. Whereas Mount McLoughlin is in the more typical 50:50 range of lava flows:pyroclastics, Brown Mountain is skewed far to the lava-rich end of the spectrum. Fieldwork at Brown Mountain indicates that the proportionality is more likely 85:15 to 90:10 in favor of lavas, making Brown Mountain much more like a shield volcano than a composite volcano in that regard. Because shield volcanoes are almost invariably basaltic in chemical composition and Brown Mountain is a rather typical andesite, perhaps the best term to describe it would be "lava cone." The dearth of pyroclastics at Brown Mountain suggests the volatile content of the Brown Mountain magma was unusually low relative to other andesite occurrences. Lower volatile content would reduce the amount of effervescence as the magma reached the Earth's surface, thus diminishing the amount of pyroclastic material formed during an eruptive phase.

Oregon state highway 140 cuts across the southern segment of the Mount McLoughlin quadrangle, connecting the cities of Medford on the west to Klamath Falls on the east. This major thoroughfare provides easy access to Fish Lake and Fourmile Lake, two major recreational destinations in the quadrangle for camping, hiking, biking, boating, and fishing activities. Three U.S. Forest Service (USFS) campgrounds are located in close proximity to Fish Lake, two on the north shore of the lake and one just off road USFS 37 a mile west of the Fish Lake Dam. An additional USFS campground can be found on the southwest shore of Fourmile Lake. Access for boats is provided at both lakes. A small store and restaurant are available at the Fish Lake Resort, where hot showers are available for a fee. The Resort is located immediately adjacent to one of the USFS campgrounds on Fish Lake. The Pacific Crest Trail (PCT; see Figures 8A and B) passes within two miles of the Fish Lake Resort, which makes the resort a convenient spot for through-going hikers on the PCT to resupply, pick up mail and packages, and have a good meal plus a shower. It is particularly convenient in this instance because a network of hiking and

biking trails connects the USFS campgrounds at Fish Lake with those at the much larger recreation areas at Lake of the Woods, which is located 6 miles east of Fish Lake, thus forming a major trail intersection 2 miles east of Fish Lake (see following web address for more information: <http://www.traveloregon.com/Explore-Oregon/Southern-Oregon/Outdoor-Recreation/Bike-Oregon/Mountain-Biking/Brown-Mountain-Trail.aspx>). The PCT cuts across the Mount McLoughlin quadrangle in a north-south orientation passing between Fourmile Lake and Mount McLoughlin, crossing state highway 140, and wrapping around Brown Mountain on its west side (see the following web address for more information: http://www.pcta.org/about_trail/overview/oregon.asp). The PCT provides the best access to areas immediately adjacent to both Mount McLoughlin and Brown Mountain.

The Mount McLoughlin quadrangle encompasses the southern termination of the Sky Lakes Wilderness, which also includes Mount McLoughlin (see the following web address for more information: http://www.fs.fed.us/r6/rogue/wilderness_skylakes.html). For a reasonably fit individual no visit to southern Oregon is complete without a day trip to climb Mount McLoughlin. Information about doing so is available from a number of web sites (e.g., http://www.fs.fed.us/r6/rogue/trails_mcloughlin.html). Having climbed Mount McLoughlin on a number of occasions, the most recent being in July of 2009, I thought a thumbnail sketch of such a climb might be insightful.

From state highway 140 turn north on to the gravel but well-maintained access road to Fourmile Lake (USFS road 3661). Approximately 3 miles up the road turn left (west) at a well-marked intersection that in approximately 0.5 miles arrives at a parking lot situated at the Mount McLoughlin trailhead. This is a USFS fee area, so there is a \$5 per day charge for parking. Envelopes are provided at the trailhead, or you can purchase a parking permit ahead of time at the Fremont-Winema USFS Office in Klamath Falls. Check the weather before setting out on the trail, and be sure to have a sturdy pair of hiking boots/shoes, a camera, mosquito repellent, and an ample supply of liquids with you as there is no potable water available along the trail. The mosquito repellent is keenly important early in the summer through August, especially in the morning when the mosquitoes are particularly voracious.

As you cross the Cascade Canal that flows immediately adjacent to the gravel parking lot, make sure to register in the ledger provided (see Figures 9A through 9D). Once on the trail and keeping a reasonable pace it should take approximately 4 to 4.5 hours to reach the summit. The trail climbing the peak is well marked with white/blue splats of paint on boulders and outcrops plus in some places on remnants of old telephone line that once extended up to a now removed fire lookout building. Climbing steadily upward and going around, over, and between boulders that are part of blocky basaltic andesite lava flows that form the cone shape of Mount McLoughlin (see Figure 10) a sharp ridge is reached that forms a very steep slope that faces to the east and north. Reaching this spot provides a respite from the mosquitoes as well as a clear view of the trail to the summit and a spectacular panorama out to the east toward Fourmile Lake and Pelican Butte (see Figures 11A and 11B).

The ridge was formed as a result of a large catastrophic landslide that occurred several tens of thousands of years ago, very likely at a time of glaciation when summer melting would produce much meltwater to interact with the relatively weak hydrothermally altered volcanic rock that characterizes the central cone area of composite volcanoes at a very shallow depth (Cas and Wright, 1987; Bardintzeff and McBirney, 2000). Perhaps the triggering event was an earthquake not unlike those that shook the area in 1993 (see Figure 1). The result is as if a large ice-cream

scoop had been employed on the northeast side of the volcano, leaving behind an arcuate horseshoe-shaped, steep-walled depression lined with angular and unsorted volcanic debris, somewhat similar in physical appearance to Mount Saint Helens after that volcano's May 18, 1980 eruption except that there is little evidence to suggest a volcanic eruption was involved with the catastrophic landslide at Mount McLoughlin. From here on, the path to the summit of Mount McLoughlin is along the ridge edge.

Once at the summit, panoramic views abound. Large blocks of the youngest basaltic andesite lava flow to emanate from the summit crater form a capping layer at the top of the peak with the blocks often tinged with yellow from late-formed sulfur that sublimated from ancient fumaroles (see Figure 12). South Squaw Tip and North Squaw Tip, two parasitic volcanic vents on the west slope of Mount McLoughlin, are readily visible from the summit (see Figure 13). On your way down, keep to the ridge crest, essentially retracing your steps back to the point where you initially crested the ridge. Do not succumb to the temptation to "boot ski" down any of the snowfields that might remain on the slopes of the volcano. Doing so will lead you into very thick intergrowths of brush and young trees that would make for a very arduous and circuitous hike back to the trailhead or, worse yet, to state highway 140. Lastly, be alert for loose rock fragments on the way down as they make it relatively easy to slip, slide, and fall. The hike back to the trailhead can be completed in 2 to 2.5 hours, and the Cascade Canal might be an inviting place to rest your weary feet in for a few minutes once the end of the trail is reached.

The Cascade Canal was constructed in early twentieth century to bring surface water from the Klamath River drainage basin into that of the Rogue River to add to the Medford water supply. Two web sites (<http://www.rrvid.org/MN.asp?pg=history> and <http://www.talentid.org/mn.asp?pg=DistrictHistory>) provide a history of irrigation in southwestern Oregon and of the quest for additional supplies of water that led to dam and canal construction. Fourmile Lake and Fish Lake are the two foremost destinations in the Mount McLoughlin quadrangle for weekenders and vacationers who are interested in camping, fishing, boating, hiking, and biking. With the Fish Lake Resort providing a small restaurant and store for essential groceries plus hot showers for a fee and a laundry facility, it is a mecca to those using the outdoor recreation venues available in the immediate area.

Both Fourmile Lake and Fish Lake are reservoirs impounded behind earthen/rock dams. Figures 14A and 14B are images of Fourmile Lake; Figures 15A and 15B are of the dam itself. The siphon depicted in Figure 15B takes water from Fourmile Lake into a fixed diameter pipe that empties into the Cascade Canal, which is an unlined, approximately 1-m deep by 3-m wide ditch. Figures 16A and 16B are photos of the canal; the former was taken at the upstream end near Fourmile Lake, while the latter is from near the parking lot for the Mount McLoughlin trailhead. Some water is lost from the canal due to evaporation and soaking into the porous and permeable volcanic soil. Small streams emptying into the canal make up for some of that water loss. The water transported by the Cascade Canal ends up in Fish Lake, which is in the Rogue River drainage basin, while the water collected into Fourmile Lake is in the Klamath River drainage basin. Unsurprisingly, when water leaves one drainage basin for another, particularly in the western United States, issues are going to arise. Taking water from the Klamath drainage and transferring it to the Rogue River drainage is no exception. For one glimpse into the debate, see the report "Water imports and exports between the Rogue and Upper Klamath Basins," prepared for the Klamath Alternative Dispute Resolution Hydrology Steering committee by Jonathon L. La Marche (unpublished, 2001, 7 p.).

Fish Lake is the smaller of the two reservoirs, and a view of it is provided in Figure 17, while Figures 18A and 18B are of the dam itself. The siphon depicted in Figure 18B takes water from Fish Lake into a fixed diameter pipe that carries it to the North Fork of the Little Butte Creek. Figure 19A depicts Fish Lake water exiting the siphon at the headwaters with Robinson Butte, a Late Pleistocene basaltic scoria cone complex, as the backdrop, while Figure 19B is a bucolic scene a few hundred meters downstream from the dam. This water is now on its way westward to the Ashland-Medford valley and its growing urban population.

There are two currently inactive hard-rock quarries within the boundaries of the Mount McLoughlin quadrangle and no cinder pits. One quarry site is immediately adjacent to the Fish Lake Dam where, on the south side, a Brown Mountain blocky andesite flow was used as the source for the large blocks composing the core of the dam. Figure 20 provides a view of what the lava flow surface looks like, a beautiful blocky flow, and Figure 21A depicts the 15-m-high quarry wall that provides a cross-sectional view of the blocky lava interior. Figure 21B shows a close-up of the interior 5 to 8 m below the surface. As a lava flow cools from the outside surface inward, its interior continues to move until the viscosity becomes so high that gravity is unable to overcome the resistance and that layer freezes in place. Warmer layers to the interior continue to move until they too cool sufficiently and freeze in place like a stack of playing cards. This petrologic feature is called platy flow jointing. In the case of blocky andesite lava flows, individual “playing cards”/tabular lava “plates” range between 2 and 10 cm in thickness and can be used as paving stones or stacked to build fire pits and fences or for other more decorative purposes.

The second inactive quarry site is in Public Land Survey System (PLSS) section 20 on the far west-central margin of the Mount McLoughlin quadrangle. This particular site has been the source of an extensive amount of road-building material. A broad view of the quarry is provided in Figure 22 with Mount McLoughlin and North Squaw Tip providing the scenic backdrop. Figure 23A provides a closer look at the rock-forming lava flow material and its well-developed platy jointed nature, which greatly facilitates its crushing. Close examination (see Figure 23B) of a representative hand sample easily demonstrates why this lava’s mineralogy is unique in the Mount McLoughlin quadrangle. The common amphibole hornblende forms elongate tabular phenocrysts that make this lava flow distinguishable from all the others present in the area.

Before initiating a broad examination of the geology of the Mount McLoughlin quadrangle, a comment on rock nomenclature is in order. When geoscientists classify igneous rock samples they often come at it from two points of view. One is based on identifying the visible minerals in a hand sample (a modal mineral classification), and the other is based on a chemical analysis of that sample (a chemical classification of igneous rocks – see Figure 24 as an example). The latter method is more precise and rigorous, and the former is less precise and is open to more opinions. The most common volcanic rocks (basalt, basaltic andesite, andesite, dacite, rhyolite) define a sequence in which the iron- and magnesium-bearing silicate minerals (olivine, orthopyroxene, clinopyroxene, hornblende, biotite) are most abundant on the left side of the sequence, forming upward of 50 to 60 percent of the minerals present, and decrease to nearly zero to the right, namely, in rhyolite. The remaining 40 to 50 percent of the rock consists mostly of plagioclase feldspar, a non-iron- or -magnesium-bearing silicate mineral, plus a few percent of chromium, iron, and titanium dominated oxide minerals. With regard to rock chemistry, silica (SiO_2) increases from basalt to rhyolite and correlates directly with increasing viscosity and greater explosivity.

Table 1, which accompanies the geologic map of the Mount McLoughlin quadrangle, contains chemical and age data for all analyzed rock samples. Figure 1 also depicts the location of the samples for which age dates exist, both within the Mount McLoughlin quadrangle and immediately adjacent to it. These adjacent radiometrically dated sample locations are depicted because they are from extensions of the volcanic rock units found within the Mount McLoughlin map area. The goal was to show all the dated sample locations for each volcanic unit discussed in the Explanation of Map Units. Figure 24 is a total alkali ($\text{Na}_2\text{O} + \text{K}_2\text{O}$) versus SiO_2 diagram that summarizes the rock names that are most germane for the volcanic materials present in this quadrangle. In addition, the chemical data are displayed for each stratigraphic unit that is defined below using an individualized symbol that is summarized in the legend that accompanies Figure 24. Lastly, Mertzman (2000) and Mertzman (unpublished data, 2007 and 2008) provide many new age dates, derived from both a whole rock K-Ar method and $^{40}\text{Ar}/^{39}\text{Ar}$ technology, that have been measured through August, 2009. Radiometric age dates derived from samples located within the Mount McLoughlin quadrangle are summarized in a histogram depicted in Figure 25A, while Figure 25B compiles all the age data from the Mount McLoughlin and its adjoining eight quadrangles to provide a framework for comparison. No vestige of the Early or Late Western Cascade volcanic episodes is exposed in the Mount McLoughlin quadrangle. Due west, however, and not very far into the eastern portion of the Willow Lake quadrangle, rocks of the lower Miocene Heppsie Formation crop out. Corroborating age date data are clearly depicted in Figure 25B. An age gap in volcanic activity of approximately 13 million years separates Heppsie Formation with the onset of Early High Cascade volcanic activity that is well represented in the Mount McLoughlin quadrangle. Farther to the south in the Mule Hill quadrangle (Mertzman and others, 2008), Late Western Cascade volcanic activity is quite apparent, but clearly it dies out farther to the north.

Finally, before embarking on a description of the stratigraphic units contained within the Mount McLoughlin quadrangle, it is well worth noting the kaleidoscope of volcanic rocks that were formed and extruded on to the Earth's surface in this small area of the Cascade Mountains during the Upper Miocene (7.246 to 5.332 Ma, Gradstein and others, 2004). In addition to the Basalt of Rye Flat that contains two varieties of basalt described below and the Basaltic Andesite of Dogwood Spring that contains three varieties of basaltic andesite, also described below, Mertzman and others (2007) in the Brown Mountain quadrangle and Mertzman and others (2009) in the Robinson Butte quadrangle described the Basalt of Pole Bridge Creek that contains two varieties of trachybasalt with quite unusual geochemistry. The region of magma generation beneath this relatively small area that encompasses portions of these three juxtaposed quadrangles (see Figure 1) must be quite heterogeneous in composition given that this diverse array of mafic volcanic rocks was generated nearly simultaneously in Earth's history.

Explanation of Map Units

Qal Alluvium (Holocene)—Unconsolidated sediment found in close proximity to modern drainages.

Qg Undifferentiated colluvium and alluvium (Pleistocene to Holocene)—Two distinct erosional processes have created a complex sedimentological situation on the northeast flank of Mount McLoughlin: glacial and mass wasting by landslides. Because the glacial and landslide sediments have been highly intermixed and are only locally distinguishable, they are combined stratigraphically and spatially into this single unit. Nevertheless, the two processes are discussed separately below.

Glacial erosion: Small lakes and ponds, some of them ephemeral, are concentrated in the northeast corner of the map, with Freye Lake being one of the larger natural lakes in the Mount McLoughlin quadrangle (see the geologic map and Figure 26). This hummocky terrain is composed of unconsolidated multi-lithologic sediment the origin of which seems much more related to glacial activity than any other geologic process. Some of the sediment seems to be morainic in origin (poorly sorted, boulder- to clay-sized material composed of several lithologies) with small bodies of water impounded in small basinlike topographic features or perhaps behind low walls of debris. Are they kettles of various dimensions formed by melting blocks of ice brought down hill by the landslide? Perhaps they have a more benign glacial origin unrelated to the landslide, but that becomes more difficult to believe given the relatively low elevation (6,000 to 6,500 feet) of the features.

Landslide mass wasting: Forming the topographically dominant feature in the quadrangle, Mount McLoughlin appears as the quintessential example of a composite volcano when viewed from the west or the south. It appears beautifully symmetric—not all that different from Mount Fuji in Japan. However, when viewed from the north or east, it is clear that some event has occurred that greatly modified its original conical appearance (see Figure 27). Reconstructing past events is never easy, but in this instance a reasonable hypothesis is easy to fashion because of the inherent structural weakness of the central cone area, which is due to pervasive hydrothermal and fumarole activity in the summit area of composite volcanoes. The coupling of alpine glaciation and its annual spring and summer meltwater has set the geologic stage for massive landslides *if* triggering events of sufficient magnitude were to happen at times when all the other structural factors related to cohesion have been minimized. Walking the PCT segment from Freye Lake north to where the trail originating from Fourmile Lake connects into the PCT, a sharp boundary is reached where scattered meter-wide boulders are encountered sitting on the countryside like golf balls or Easter eggs (see Figures 28A and 28B). The boulders, in terms of their compositions, are randomly scattered across this landslide area: some are blocks from lava flows and quite pristine in terms of original mineral preservation, some are blocks of vent agglomerate, and some blocks are highly oxidized with encrustations of sulfur—in other words, they form a hodge-podge.

Volcanic Rocks

Qbv Basaltic/basaltic andesite/andesite vent deposits (Pleistocene)—Poorly lithified to unconsolidated lapilli- to ash-sized cinders, black to brown to red with lesser amounts of similarly colored lava spatter, bombs, and scoria. These deposits mark volcanic vent areas that are often cinder cones.

Qabm Andesite of Brown Mountain (Upper Pleistocene)—At summit elevations of 7,311 feet for Brown Mountain and 9,495 feet for Mount McLoughlin, both Late Pleistocene andesite composite volcanoes, these edifices dominate the topography of the surrounding area (see Figure 5). Mount McLoughlin exhibits quite well the primary characteristic that defines a composite volcano: alternating layers of lava flows and pyroclastics (see Figures 3 and 10). On the other hand, Brown Mountain is unusual in that it consists of a much higher volume of lava and a relatively meager amount of pyroclastic material compared to many other andesite volcanoes. Young blocky andesite Qabm lava flows that have meager amounts of vegetative cover are prominent in the southeast corner of the Mount McLoughlin quadrangle. On a freshly broken rock surface the Brown Mountain lava is dark gray and is highlighted by the lack of phenocrysts (see Figure 7, left-hand specimen). All visible crystals are ≤ 1 mm in diameter. Plagioclase, which constitutes nearly 75 percent of the total rock sample, is the dominant mineral present followed orthopyroxene and clinopyroxene. Examining thin sections shows that many of the small plagioclase phenocrysts have resorbed core areas surrounded by relatively thick unaltered plagioclase rims or coronas (see Figure 29). Pressure release as magma perhaps moved from somewhere deeper in the crust to the surface following a more or less adiabatic pressure-temperature path could lead to a rise in temperature and resorption of the plagioclase core regions (McBirney, 2007). Orthopyroxene is much more abundant than clinopyroxene and forms 0.5- to 0.8-mm-long elongate rectangles, the feathery terminations of which indicate relatively rapid cooling of the lava (see Figures 30A and 30B) (Philpotts, 1989). Only minor to trace amounts of olivine, titanomagnetite, apatite, and matrix glass are present. Two pieces of strontium isotope data are available for Brown Mountain samples 84-13 and 84-58. These samples have $^{87}\text{Sr}/^{86}\text{Sr}$ ratios of 0.703667 ± 6 and 0.703664 ± 8 , respectively, values so similar that they suggest the two lavas were subject to virtually identical origins (Mertzman, unpublished data). No K-Ar age is available for this unit due to its youthfulness. Field evidence suggests the oldest lavas may be on the order of 50,000 to 75,000 years old with the youngest being on the order of 20,000 to 25,000 years old.

Qbrb Basalt of Robinson Butte (Middle Pleistocene)—Light gray to dark bluish-gray in hand sample color, lava samples are consistently lighter in color than that of pyroclastic samples. Robinson Butte cinder/scoria cone, the source of these lavas, is located in the extreme northeast corner of the Robinson Butte quadrangle (Mertzman and others, 2009). Three- to five-meter thick lava flows with pahoehoe surfaces are abundant. Vesicles 5 to 10 mm long, stretched out in the direction of flow, and partially lined with vapor-phase-deposited secondary minerals are common. The lava flows are only vaguely diktytaxitic in nature, most likely due to the slightly higher silica content (~50 to 52 percent SiO_2). The lavas have a glomeroporphyritic texture with olivine (1 to 3 mm in maximum dimension), often distinctly rimmed with

low-temperature iddingsite alteration, constituting 10 to 15 percent of each hand sample. Poikilitic within early-formed olivine crystals are chrome-spinel inclusions. Abundant clinopyroxene (1 to 3 mm) and plagioclase (0.5 to 1 mm) phenocrysts constitute nearly 50 percent of a hand sample and are present as individual crystals as well as in glomeroporphyritic clumps. Several percent of the plagioclase phenocrysts present in the Robinson Butte basaltic lavas have a strikingly different appearance than the vast majority of plagioclase crystals in that the crystals have been strongly resorbed into a fine-grained crystalline aggregate such that only thin rims of unaltered later-formed plagioclase remain. These severely altered phenocrysts could be xenocrysts, that is, foreign crystals entrained by the rising Robinson Butte magma on its way to the surface. The groundmass is primarily intergranular to subophitic in nature. One whole-rock K-Ar age, 0.40 ± 0.30 Ma, is available for this unit, measured on a sample from the southerly adjacent Brown Mountain quadrangle. One $^{40}\text{Ar}/^{39}\text{Ar}$ age has been recently determined on sample 00-67 from the Robinson Butte quadrangle and is preferable because of its much better precision. Robinson Butte volcanic activity is 0.36 ± 0.06 Ma.

Qbam Basaltic Andesite of Mount McLoughlin (Middle to Upper Pleistocene)— Mount McLoughlin is a composite volcano where exposure of the cone-forming lavas is much better than what is typical for composite volcanoes due to the massive landslide described above. A stratigraphic sequence of lavas was collected from the top of the peak down through as many lava flows as could safely be reached (see samples 84-38 through 84-48 in Table 1 and on the geologic map). What clearly became evident when the hand samples were placed side by side in order from youngest at the top to oldest at the bottom is that there was little change in petrographic character through the youngest five samples of cone-building lava flows. The older five are somewhat less porphyritic, but viewing Table 1 indicates virtually no change in major and trace element geochemistry through the entire stack of ten lava flows. The mineralogy (plagioclase, orthopyroxene, clinopyroxene, olivine, and titanomagnetite in order of decreasing modal abundance) is the same through all ten lava flows; what has changed is the magma cooling history that, as a function of decreasing age, has led to increasing phenocryst size. As is depicted in Figure 6, Mount McLoughlin lavas are distinctly porphyritic in texture even in the most pyroclastic of samples. Singular crystals 1 to 5 mm in diameter and glomeroporphyritic clumps up to nearly 1 cm characterize between a quarter and 40 percent of a given hand specimen. Plagioclase phenocrysts form 25 to 30 percent of a typical hand specimen, while pyroxene forms 5 to 8 percent and olivine constitutes 2 to 5 percent. The glomeroporphyritic clumps that are dominated by ferromagnesian minerals when viewed in the lighter colored interior portions of lava flows look spotted in nature (see Figure 6, right-hand specimen). The rock is best classified as basaltic andesite porphyry. The term “multiply saturated” is used to describe a rock in which several minerals form phenocrysts and are modally abundant. Figures 31A and 31B (same image, uncrossed and crossed polarizers) and Figure 32 depict large phenocrysts of orthopyroxene that have grown around already formed crystals of clinopyroxene, olivine, and plagioclase. The textural term for this relationship is poikilitic. The clinopyroxene and olivine had already crystallized and grown to their maximum size before the advent of significant orthopyroxene crystallization. Poikilitic relationships are instrumental in determining the sequence of crystallization that has taken place in the formation of rocks. In the Mount McLoughlin lava flows, olivine, plagioclase, and clinopyroxene crystallized before and during orthopyroxene growth. Plagioclase

phenocrysts are chemically zoned, primarily in a normal manner; that is, the high-temperature, more calcium-rich component is concentrated in the center of the crystal, while the lower-temperature, more sodium-rich component is concentrated at the margin of the crystal (see Figures 33A and 33B). McCanta and others (2007) and Rutherford (2008) described how changes that take place at the edges of phenocrysts during magma ascent and the concomitant loss of volatiles can be used in some situations to quantify the rate at which the ascent occurred. Olivine (2 to 5 percent) is a relatively minor but pervasive modal constituent in the Mount McLoughlin lava flows. In numerous instances olivine has thin reaction rims indicating that olivine had reached its lower limit of temperature stability and had begun to react with the surrounding magma and form orthopyroxene around the margins of the earlier-formed olivine crystals (see Figures 34A and 34B). This well-known and widely encountered chemical reaction is often a characteristic of basalt, basaltic andesite, and even some andesite volcanoes associated with convergent plate boundaries (Winter, 2010; McBirney, 2007). Two pieces of strontium isotope data are available for Mount McLoughlin samples 84-38 (summit sample) and 84-48 (lowest elevation sample). These samples have $^{87}\text{Sr}/^{86}\text{Sr}$ ratios of 0.703226 ± 8 and 0.703258 ± 6 , respectively, values so similar that they suggest the two lavas were subject to virtually identical origins (Mertzman, unpublished data). The Brown Mountain strontium isotope data are significantly different from those of Mount McLoughlin, suggesting somewhat different magma source rocks and/or different magma evolutionary histories. Five whole-rock K-Ar dates are available for this unit (see samples KWW25-9, 84-48, 84-38, 91-49, and 91-52); the ages measured were 0.66 ± 0.02 Ma, $< 150,000$ years, 0.08 ± 0.03 Ma, 0.05 ± 0.03 Ma, and 0.08 ± 0.03 Ma, respectively. The first sample is located in the Willow Lake quadrangle, and the latter four samples are located in the Mount McLoughlin quadrangle.

Qbwl Basalt of Woodpecker Lake (Lower Pleistocene)—To the north and east of Fourmile Lake and west of Long Lake in the northwest corner of the Lake of the Woods North quadrangle are a number of small basalt scoria and cinder cones. These have been placed together in this unit because of relatively similar mineralogy and chemistry. This unit has also been truncated by north-south oriented faults. The color of these rocks is variable from a tan-gray combination (mostly vesicle-free lavas) to a medium gray to a quite dark blue-gray (quite vesicular pyroclastic material or flow top). Some of the lavas contain 8 to 10 percent green olivine phenocrysts, 1 to 4 mm in diameter, with little alteration to iddingsite and only 1 to 2 percent plagioclase, 1 to 2 mm in diameter. On the other hand, several flows have nearly equal amounts of olivine and plagioclase phenocrysts. Pyroxene is always confined to the matrix. Three whole-rock K-Ar ages are available for this unit (see samples BS92-77, 96-11, and 96-13); the measured ages were 1.12 ± 0.05 Ma, 1.23 ± 0.08 Ma, and 1.32 ± 0.08 Ma, respectively. Sample BS92-77 is located in the Lake of the Woods North quadrangle. The other two samples were collected northeast of the Mount McLoughlin quadrangle in the Pelican Butte quadrangle.

Tpbbl Basalt of Blue Canyon Lake (Upper Pliocene to Lower Pleistocene)—To the north and west of Fourmile Lake in the northeast corner of the Mount McLoughlin quadrangle extending northward into the Rustler Peak quadrangle is a series of small shield volcanoes (see Smith Rock [Figure 35], Blue Rock, and Cat Hill that extruded quite similar basalt during the time interval 2.0 Ma to 1.7 Ma). With approximately

equal amounts of small ~1 mm phenocrysts of olivine and plagioclase, totaling 15 to 20 percent of a hand-sized specimen, set in a finer-grained matrix dominated by plagioclase and pyroxene, the Basalt of Blue Canyon Lake is a rather main-stream high-alumina basalt (Winter, 2010; McBirney, 2007). Figures 36A and 36B document the reaction relationship between olivine and magma to form a corona of orthopyroxene that grows larger over time as long as the temperature of the magma body decreases slowly. The potential is there for some or all of the olivine to react out with the magma and virtually wipe the slate clean so to speak, erasing most if not all the evidence that olivine was ever a crystallizing mineral phase in the magma. Figure 37 documents a second behavior of olivine, and that involves its relationship with oxygen. Olivine contains iron only in the ferrous (Fe^{+2}) state, so when magma moves very close to or at the Earth's surface and gains access to the atmosphere and its nearly 21 percent O_2 content, the olivine will suffer high-temperature oxidation from the perimeter of the crystal inward over time (Haggerty and Baker, 1967). The two olivine crystals shown in Figure 37 also show evidence of low-temperature oxidation. The yellow-brown coloration that follows the curving fracture traces through the crystals indicates the presence of the mineral assemblage iddingsite, a low-temperature alteration product of olivine (Philpotts, 1989; Baker and Haggerty, 1967). One whole-rock K-Ar date and one $^{40}\text{Ar}/^{39}\text{Ar}$ date are available for this unit (see samples 92-66 and 06SM-55); the ages measured were 1.76 ± 0.08 Ma and 1.96 ± 0.03 Ma, respectively. The former sample is located in the Mount McLoughlin quadrangle, while the latter sample is from the Rustler Peak quadrangle, more specifically from the feature known as Smith Rock.

Tpbaf Basaltic Andesite of Freye Lake (Upper Pliocene)—Freye Lake itself is located in the east-central part of the Mount McLoughlin quadrangle, which is located due west of the Lake of the Woods North quadrangle. This unit is a harbinger of things to come in this general area in that its physical appearance on a fresh unweathered rock surface is similar to the lavas from the Late Pleistocene Mount McLoughlin volcano. These medium gray lavas have 30 to 40 percent phenocrysts ranging from 1 to 3 mm in diameter. Plagioclase feldspar is the most abundant mineral, followed by clinopyroxene, olivine, and orthopyroxene. Together these three mafic minerals constitute 10 to 15 percent of the phenocrysts, which are seen individually as well as in clumps of all three mafic minerals together with plagioclase. Surrounding the phenocrysts is a gray matrix that is dominated by fine-grained, flow-aligned plagioclase crystals with some scattered Fe-Ti oxide crystals (titanomagnetite?). One piece of strontium isotope data is available for Basaltic Andesite of Freye Lake, on sample 84-50. This sample has an $^{87}\text{Sr}/^{86}\text{Sr}$ ratio of 0.703669 ± 7 , a value indistinguishable from the Brown Mountain samples and considerably higher than the Mount McLoughlin samples. Given the virtual identicalness of the mineralogy and the subtle distinctions in geochemistry between the Basaltic Andesite of Freye Lake and the Basaltic Andesite of Mount McLoughlin, the magnitude of the strontium isotope difference is surprising. One whole-rock K-Ar age is available for this unit (see sample 84-50); the age determined was 2.42 ± 0.15 Ma. Sample 84-50 is located within the Mount McLoughlin quadrangle.

Tpbad Basaltic Andesite of Dry Creek (Middle Pliocene)—On the outcrop, the Basalt of Dry Creek is noteworthy for its well-developed spheroidal boulders, a product of long-term mechanical and chemical weathering of well-jointed igneous rock (see

Figure 38 for an example). Obtaining a fresh unweathered representative hand-sized sample specimen can be a challenge given the rounded exfoliating nature of the boulders. Examining first a rock sample of the Basalt of Dry Creek with a hand lens and then a thin section with a petrographic microscope shows distinctive 2-5 mm in diameter glomeroporphyritic clumps of lathlike plagioclase feldspar phenocrysts together with olivine and clinopyroxene (see Figure 39). Phenocrysts constitute 30 to 40 percent of a fresh unweathered rock surface with plagioclase > olivine \leq clinopyroxene. The phenocrysts range from 1 to 3 mm in diameter and are found individually as well as in clumps. Olivine has been substantially altered to iddingsite (see Figure 39). Large, chemically zoned clinopyroxenes, often twinned by the Carlsbad law, make this basalt unit quite distinctive (see Figures 40A and 40B). The margins of the clinopyroxene crystals are marginally resorbed, probably a result of changing physical conditions from the point where the clinopyroxene crystallized to the point where the lava was extruded on the surface of the Earth (see Figure 41). Olivine and clinopyroxene together constitute 8 to 10 percent of the phenocryst mineralogy. The fine-grained gray matrix that constitutes nearly two thirds of the lava is dominated by plagioclase and pyroxene and has scattered pinhead sized vesicles present. Well-developed spheroidally weathered cobbles and boulders characterize outcrops of this unit along Oregon State Highway 140. Two whole-rock K-Ar ages are available for this unit (see samples 14K-91 and 84-62); the ages determined were 3.43 ± 0.06 Ma and 3.14 ± 0.07 Ma, respectively. The former sample is located within the Mount McLoughlin quadrangle, while the latter is from the Lake of the Woods North quadrangle (see Figure 1).

Tpafi Andesite of Fish Lake (Lower Pliocene to Lower Pleistocene)—This unit primarily consists of andesite lava flows, but intercalated among the andesite flows are more mafic flows of basaltic andesite, much like the Andesite of Ichabod Spring. These andesites are quite porphyritic with plagioclase phenocrysts, singularly and in glomeroporphyritic clumps up to 7 and 8 mm in diameter, that amount to between 30 and 40 percent of a typical hand specimen. Both orthopyroxene and clinopyroxene are present, usually amounting to 5 to 7 percent of the hand sample. Olivine is absent or is present at a level of no more than 1 to 2 percent. On the whole, outcrops of this unit are relatively limited, and iron staining in and along fracture surfaces that pass through the rock leaves the impression that the rock is highly weathered. No vents for these lavas were discovered. Three whole-rock K-Ar ages are available for this unit: 3.97 ± 0.08 Ma, 3.56 ± 0.06 Ma, and 1.67 ± 0.03 Ma. All three of these samples, HC91-44, HC91-67, and HC91-49A respectively, are located within the Mount McLoughlin quadrangle.

Tmbrf Basalt of Rye Flat (Upper Miocene)—The immediate summit area of the Rye Flat shield volcano has a carapace of younger Basaltic Andesite of Dogwood Spring lava, and its northern and eastern flanks have been partially enveloped by younger lavas, particularly those from Mount McLoughlin. Figure 42 provides a very clear sense of the relationship. Driving east on Oregon highway 140 from Medford and White City following the drainage of the North Fork of the Little Butte Creek (see Figure 1), nearing the boundary between the Willow Lake and the Mount McLoughlin quadrangles, the outcrop pattern changes rather dramatically from predominantly fragmental volcanic material of the Heppsie Formation to massive lava flows that are part of the Basalt of Rye Flat (see Figures 43 and 44). These outcrops extend for

approximately 2 miles on the north side of the road until the turnoff to Jackson county road 821 to Butte Falls. Several outcrops display well-formed columnar jointing (see Figure 44) and channel fill morphology (see Figure 45A), whereas others expose pyroclastic materials that covered the areas between basalt lava flows (see Figure 45B). Hand samples of Basalt of Rye Flat are gray and aphanitic in texture with the largest phenocrysts being 1 to 1.5 mm in maximum diameter. Greenish to iridescent olivine is the most visible mineral in hand sample, present at the 2 to 5 percent level. In thin section olivine contains small dark subhedral to euhedral spinel crystals, the first mineral to crystallize from the Rye Flat basalt magma (see Figure 46A). The olivine has been substantially altered to iddingsite by low-temperature oxidation and hydration (Baker and Haggerty, 1967). These olivine phenocrysts reside in a finer-grained matrix that is composed of primarily plagioclase and pyroxene with a few scattered small olivine crystals. Plagioclase, present as elongate tabular crystals rather than in a more equi-dimensional form due to rapid cooling (Winter, 2010), depicts a well-developed flow-aligned texture that documents movement in the lava before complete solidification (see Figure 46B). This flowage pattern, like water around pebbles in a stream, is known as a trachytic texture (Philpotts, 1989). Basalt of Rye Flat comes in two geochemical “flavors”: one is much higher in MgO and lower in Al₂O₃ and K₂O, reflecting a considerably higher olivine content, while the second and more abundant type has lower MgO and higher Al₂O₃ and K₂O, reflecting the presence of significantly less olivine. Two whole-rock K-Ar ages are available for this unit: 6.11 ± 0.21 Ma, 6.06 ± 0.10 Ma. These two samples, 91-60 and JB91-41, respectively, are located in the adjoining Willow Lake quadrangle.

Tmbads Basaltic Andesite of Dogwood Spring (Upper Miocene)—In sharp contrast to the massive outpourings of basalt lava flows that characterize Basalt of Rye Flat, Basaltic Andesite of Dogwood Spring lava flows are commonly denoted by spheroidally weathered channel-fill structures (see Figure 47A) and relatively thin (2 to 3 m) lava flows that invariably have well-developed platy jointing (see Figure 47B). There are three “flavors” or petrographic varieties of basaltic andesite within this stratigraphic unit: a variety with olivine phenocrysts encased in a fine-grained matrix composed of primarily plagioclase and pyroxene, a variety with less modal olivine that has reaction rims of pyroxene that coexist with phenocrysts of plagioclase and pyroxene as individual crystals as well as in glomeroporphyritic clumps that are encased in a fine-grained matrix dominated by additional plagioclase and pyroxene, and a third variety in which the amphibole hornblende is a significant phenocryst-forming mineral (see Figure 23B for a photograph of a typical hand specimen). This third variety of basaltic andesite is interesting because hornblende is infrequently encountered in the lavas of the High Cascade volcanoes (McBirney, 2007). What makes this variety even more interesting is the coexistence of hornblende with olivine. Olivine is an anhydrous higher-temperature ferromagnesian mineral, whereas hornblende is a hydrous somewhat lower temperature ferromagnesian mineral. Significant water pressure (P_{H_2O}) is required to stabilize hornblende. Imagine a geological situation akin to a pressure cooker. Under conditions of elevated water pressure, hornblende is stable, but once the water pressure is released (imagine a body of magma moving through a portion of the crust toward the Earth’s surface) hornblende begins to react with the surrounding magma through a dehydration chemical reaction such as: **hornblende** \Rightarrow **clinopyroxene** +

orthopyroxene + plagioclase + magnetite + H₂O. A relatively fast trip from a crustal magma chamber to the surface can produce a euhedral, fine-grained pseudomorph of the original hornblende phenocryst. The very fine-grained dark material contains all the minerals to the right of the arrow in the reaction stated above (see Figure 48). For the Basaltic Andesite of Dogwood Spring, Figures 49 and 50 are telling; hornblende and olivine were at textural equilibrium, that is, both minerals were touching, sharing common grain boundaries, before the water pressure in the magma chamber was significantly reduced. Figure 51 is a cartoon of the possible pressure-temperature conditions that were in place at the time when primary hornblende and olivine coexisted together under equilibrium conditions. It suggests that olivine and hornblende were stable together at a depth of nearly 30 km (approximately 3.3 km per kilobar of pressure), perhaps somewhere near the base of the crust (Winter, 2010). Transit to the surface from this depth was, relatively speaking, quicker rather than slower given the euhedral nature of a number of the hornblende pseudomorphs (Rutherford, 2008). Five whole-rock K-Ar ages are available for Basaltic Andesite of Dogwood Spring: KWW33-91 (6.48 ± 0.10 Ma), M91-85A (6.43 ± 0.10 Ma), 84-26 (6.01 ± 0.30 Ma), 84-21 (5.97 ± 0.36), and 91-89 (5.62 ± 0.09 Ma). Samples M91-85A, 84-21, and 91-89 are located within the Mount McLoughlin quadrangle, while KWW91-33 and 84-21 are located within the adjoining Willow Lake quadrangle.

Acknowledgments. I thank Isaac Weaver for his on-going help and cheerful support in bringing this geologic map to closure. His computer skills, particularly with regard to MapInfo and Adobe Illustrator, have been particularly valuable. I also thank Karen Mertzman for all her efforts in the X-ray lab, carefully preparing and analyzing countless samples on my behalf. I thank the Keck Foundation for its generous support of the Keck Geology Consortium over the years. I thank Franklin and Marshall College for its generous support of fieldwork over the past decade that has led to the completion of this geologic map. Support from the NSF and Franklin and Marshall College to facilitate the operation of the XRF laboratory in the Earth and Environment Department is greatly appreciated.

Links

<http://www.traveloregon.com/Explore-Oregon/Southern-Oregon/Outdoor-Recreation/Bike-Oregon/Mountain-Biking/Brown-Mountain-Trail.aspx>
http://www.pcta.org/about_trail/overview/oregon.asp
http://www.fs.fed.us/r6/rogue/wilderness_skylakes.html
http://www.fs.fed.us/r6/rogue/trails_mcloughlin.html
<http://www.rrvld.org/MN.asp?pg=history>
<http://www.talentid.org/mn.asp?pg=DistrictHistory>

References

- Baker, I. and Haggerty, S. E., 1967, The alteration of olivine in basaltic and associated lavas, Part II: Intermediate and low temperature alteration: *Contr. Mineral. and Petrol.*, v. 16, p. 258-273.
- Bardintzeff, J. M., and McBirney, A. R., 2000, *Volcanology* (2nd ed.): Sudbury, Mass., Jones and Bartlett, 268 p.

- Cas, R. A. F., and Wright, J. V., 1987, *Volcanic successions*: London, Allen and Unwin, 528 p.
- Eggler, D. H., 1972, Amphibole stability in H₂O-undersaturated calc-alkaline melts: *Earth and Planet. Sci. Lett.*, v. 15, p. 28-34.
- Fisher, R. V., and Schmincke, H.-U., 1984, *Pyroclastic rocks*: Berlin/Heidelberg, Springer Verlag, 472 p.
- Gradstein, F., Ogg, J., and Smith, A., eds., 2004, *A geologic time scale 2004*: Cambridge, Cambridge University Press, xix + 589 p. + chart in folder.
- Grotzinger, J., and Jordan, T., 2010, *Understanding earth* (6th ed.): New York, W.H. Freeman, 654 p.
- Haggerty, S. E., and Baker, I., 1967, The alteration of olivine in basaltic and associated lavas, Part 1: high temperature alteration: *Contr. Mineral. and Petrol.*, v. 16, p. 233-257.
- Le Maitre, R. W., ed., 2002, *Igneous rocks: a classification and glossary of terms* (2nd ed.): Cambridge, Cambridge University Press, 252 p.
- Maynard, L. C., 1974, *Geology of Mount McLoughlin*: Eugene, Oreg., University of Oregon, M.S. thesis, 139 p.
- McBirney, A. R., 2007, *Igneous petrology* (3rd ed): Boston, Jones and Bartlett, 550 p.
- McCanta, M. C., Hammer, J. E., and Rutherford, M. J., 2007, Pre-eruptive and syn-eruptive conditions in the Black Butte, California dacite: insight into crystallization kinetics in a silicic magma system: *J. Volc. Geotherm. Res.*, v. 160, p. 263-284.
- Mertzman, S. A., 2000, K-Ar results from the southern Oregon-northern California Cascade Range: *Oregon Geology*, v. 62, p. 99-122.
- Mertzman, S. A., Hazlett, R. W., Weaver, S. G., Brackin, S., Cruz, H., Humm, A., Lunt, A., Petcovic, H., Schiffer, B., Sours-Page, R., Taylor, P., Tittler, A., and Zook, J., 2007, Preliminary geologic map of the Brown Mountain 7.5 minute quadrangle, Jackson and Klamath Counties, Oregon: Oregon Department of Geology and Mineral Industries Open-File Report O-07-09, 14 p., scale 1:24,000.
- Mertzman, S. A., Hazlett, R. W., Weaver, I. P., Crabtree, S., Eisinger, C., Gaffney, A., Gravely, D., Hall, M., Hill, M., Klawiter, B., McCreight, G., McIntosh, A., McIntosh, J., Nilsson, A., Phippen, S., Robinson, S., Sewall, J., and Winick, J., 2008, Preliminary geologic map of the Mule Hill 7.5 minute quadrangle, Klamath County, Oregon, and Siskiyou County, California: Oregon Department of Geology and Mineral Industries Open-File Report O-08-08, 37 p., scale 1:24,000.
- Mertzman, S. A., Weaver, S. G., Pasquale, S. A., Baum, J. M., and Weaver, I. P., 2009, Preliminary geologic map of the Robinson Butte 7.5 minute quadrangle, Jackson County, Oregon: Oregon Department of Geology and Mineral Industries Open-File Report O-09-02, 40 p., scale 1:24,000.
- Pacific Northwest Seismic Network. "List of magnitude 4.0 or larger earthquakes in Washington and Oregon." March 27, 2003.
http://www.ess.washington.edu/SEIS/PNSN/HIST_CAT/catalog.html (accessed 6 June 2011).
- Pacific Northwest Seismic Network. "Notable Pacific Northwest Earthquakes Since 1993 (Most Recent First)." April 30 2011.
http://www.ess.washington.edu/SEIS/EQ_Special/pnwtectonics.html (accessed 6 June 2011).
- Philpotts, A. R., 1989, *Petrography of igneous and metamorphic rocks*: Long Grove, Ill., Waveland Press, 178 p.

- Rutherford, M. J., 2008, Magma ascent rates: Reviews in Mineralogy and Geochemistry, v. 69, p. 241-271.
- U.S. Geological Survey. "Upper Klamath Basin ground-water study: Background." October 31 2008. http://or.water.usgs.gov/projs_dir/or180/background.html (accessed 6 June 2011).
- Winter, John, D., 2010, Principles of igneous and metamorphic petrology (2nd ed.): Upper Saddle River, N.J., Prentice Hall, 702 p.
- Yoder, H. S., and Tilley, C. E., 1962, Origin of basalt magmas: an experimental study of natural and synthetic rock systems: Jour. Petrol., v. 3, p. 342-532.

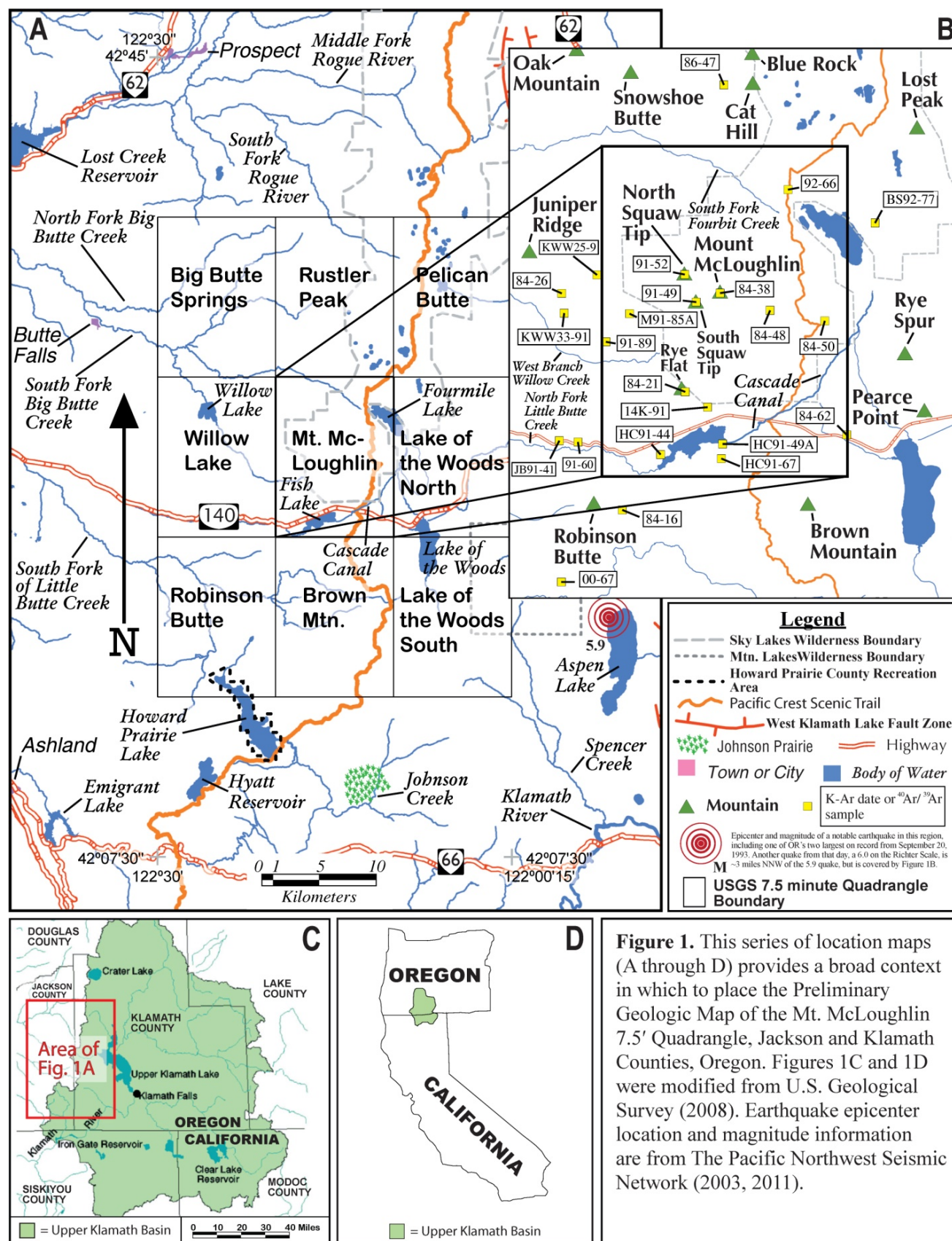


Figure 1. This series of location maps (A through D) provides a broad context in which to place the Preliminary Geologic Map of the Mt. McLoughlin 7.5' Quadrangle, Jackson and Klamath Counties, Oregon. Figures 1C and 1D were modified from U.S. Geological Survey (2008). Earthquake epicenter location and magnitude information are from The Pacific Northwest Seismic Network (2003, 2011).



Figure 2A. Looking east from the nose of a ridge south of Willow Lake, Mount McLoughlin has the classic profile of a composite or stratovolcano.



Figure 2B. Looking north from the Pacific Crest Trail as it meanders around Brown Mountain, the smooth profile of Mount McLoughlin is interrupted on its west slope by the parasitic cone South Squaw Tip.



Figure 2C. Looking south from Blue Knob provides a very different view of Mount McLoughlin. A massive landslide has exposed a cross-section of the upper portion of the volcano.



Figure 2D. Looking west from Rye Spur volcano provides a spectacular view of Mount McLoughlin and its landslide-induced topography on the north and east side of the mountain. Much of the material that broke away and slid to the northeast can be seen as the large hill to the right side of Mount McLoughlin.



Figure 3. Exposed by the landslide and located along the ridge that leads to the summit of Mount McLoughlin, a 1 to 1.5 m thick blocky lava flow inclined at 25° to 30° is seen conformably on top of a layer of coarse pyroclastic material.



Figure 4. This image of the Brown Mountain composite volcano was taken from the Seldom Creek Flats looking to the west. Whereas composite volcanoes are often thought to be a nearly 50:50 proportionality between lava flows and layers of pyroclastic material, Brown Mountain is skewed in favor of lava flows, forming a predominantly lava cone.



Figure 5. This image that encompasses both Mount McLoughlin (left) and Brown Mountain (right) was taken from the Pacific Crest Trail where it crosses the Brush Mountain – Old Baldy Ridge in the southernmost portion of the Brown Mountain quadrangle.



Figure 6. Referring back to Figure 3, the left-hand specimen was derived from the pyroclastic layer at the base of the **map tube** (0.7 m in length), while the right-hand specimen originated from the lava flow. The abundance of plagioclase phenocrysts in both specimens and the 3 to 10 mm across glomeroporphyritic clumps of olivine, orthopyroxene, and clinopyroxene (dark spots) are easy to spot.



Figure 7. A typical hand specimen of Brown Mountain lava on the left and a typical hand specimen of Mount McLoughlin lava on the right: no one will confuse the two! Whereas the Brown Mountain lava is quite aphanitic, the Mount McLoughlin is quite porphyritic with numerous crystals of light colored plagioclase feldspar and clots of dark colored ferromagnesian minerals.



Figure 8A. The Pacific Crest Trail provides access to much of the backcountry in the Sky Lakes Wilderness, of which Mount McLoughlin is an integral part.



Figure 8B. A close-up of the trail marker in Figure 8A, showing the rounded triangular insignia of the Pacific Crest Trail with Ponderosa Pine bark as a backdrop.



Figure 9A. Every adventure begins with that first step. Hiking from the Mount McLoughlin trailhead to the summit, in addition to many steps, involves an elevation gain of nearly 4,000 feet.



Figure 9B. Play it safe; be sure to sign in and out so that U.S. Forest Service personnel know at the end of the day that everybody arrived back at the trailhead safely.



Figure 9C. Sky Lakes Wilderness extends from Crater Lake National Park on the north to Oregon state highway 140 at the southern margin.



Figure 9D. The signage along both the Pacific Crest Trail and the Mount McLoughlin Trail is very natural looking and unobtrusive.



Figure 10. After you take a long uphill hike in the woods, the trees begin to thin out, and suddenly you are on a sharp ridge with a spectacular view of the remainder of the climb to the top of Mount McLoughlin. What constitutes the flanks of a composite volcano is clearly seen: interbedded thin lava flows and thick layers of pyroclastic material.



Figure 11A. From the same vantage point as Figure 10, Fourmile Lake with Pelican Butte on the horizon can be seen to the northeast. In the immediate foreground the topography extending nearly to the margin of Fourmile Lake is the result of the massive landslide that sculpted the northeast quadrant of Mount McLoughlin.



Figure 11B. The trail to the summit at times winds its way through boulders that form the tops of blocky basaltic andesite lava flows.



Figure 12. Eureka! The summit! With the foundational remains of a U.S. Forest Service fire lookout for company together with much solid outcrop of the highest stratigraphic lava flow, what a wonderful place for a well-earned snack and drink. Much of the immediate rock has yellow encrustations on it from sulfur that originated in the gaseous state from nearby fumaroles that are now extinct.



Figure 13. Nearly 2,000 feet lower in elevation but still visible from the summit is the parasitic volcano South Squaw Tip. With regard to both mineralogy and geochemistry, the lavas extruded from this parasitic volcano are absolutely identical to those that form the summit region of Mount McLoughlin.



Figure 14A. Looking out to the northwest parallel to the long axis of Fourmile Lake, remnants of Pleistocene volcanic activity form all the terrain on the horizon.



Figure 14B. In this image taken from near the Fourmile Lake Dam, with a pile of driftwood in the foreground that has accumulated due to prevailing northwest breezes, Mount McLoughlin dominates the local countryside.



Figure 15A. This image is a view of the Fourmile Lake earthen dam. Water leaves Fourmile Lake in one of two ways (excluding infiltration and evaporation): either via the concrete overflow sluiceway, which is farther to the right in the image, or through a fixed diameter pipe that supplies all the water to the Cascade Canal and that is depicted below in Figure 15B.



Figure 15B. Piles of driftwood in and around the Fourmile Lake Dam are depicted along with a fenced walkway that is joined to the dam and provides access to the submerged pipe that provides water to the Cascade Canal.



Figure 16A. Looking downstream along a portion of the Cascade Canal one mile below Fourmile Lake Dam, it flows in an approximately 3 to 4 m wide by 1 m deep trench that meanders its way to Fish Lake. An occasional down tree provides access for the hiker/geologist from one side of the Canal to the other.



Figure 16B. On steeper slopes where the water velocity is much greater, all finer-sized sediment has been eroded away, leaving a streambed formed of cobbles and boulders. The greater degree of turbulence has formed a meandering pattern of S-like bends in the Canal path.



Figure 17. Fish Lake is an artificial reservoir located in the southwest corner of the Mount McLoughlin quadrangle. It is lenticular in form, stretched out along an east-west axis. It provides a beautiful foreground for a photograph of Mount McLoughlin.



Figure 18A. The Fish Lake Dam, a predominantly boulder façade with a lining of very fine grained impermeable sediment on the reservoir side, was constructed near the headwaters of the North Fork of Little Butte Creek. Downstream of the dam the water flows west down the west flank of the Cascade Mountains to the White City – Medford area.



Figure 18B. This image captures the western tip of Fish Lake with a Brown Mountain blocky lava flow in the background and the submerged drainpipe that feeds water through the dam and into the North Fork of Little Butte Creek.



Figure 19A. This image was taken from the top of the Fish Lake Dam looking to the west down the initial few hundred meters of the North Fork of Little Butte Creek. Notice how the stream immediately begins to gently meander down the floodplain.



Figure 19B. A mile or so downstream from Fish Lake Dam, the North Fork of Little Butte Creek has broadened considerably.



Figure 20. This image is of the top of a Brown Mountain lava flow, the cross-section of which is depicted in Figures 18B and 21A. Notice the wide variability in the texture and relative smoothness of the surface of the lava flow. From a snakeskin-like mosaic pattern in the center of the image to a finer (10 to 20 cm across) blocky pattern to a typical blocky (25 to 60 cm across) flow pattern, the final appearance all depends on how the surface crust solidified and whether or not there was subsequent movement of the underlying lava. Significant movement of the hotter flow material beneath the solidified crust fractures and breaks up surficial material into a jumbled mass (Fisher and Schmincke, 1984).



Figure 21A. If you examine the far right-hand side of Figure 18B just above where the walkway connects the Fish Lake Dam to the hut on top of the concrete-encased drain, vestiges of an old rock quarry can be seen. This image is a close-up of the quarry wall whence all the rock material came to construct the Fish Lake Dam. What is being quarried is a blocky andesite flow that is part of the Upper Pleistocene Andesite of Brown Mountain. Notice the flow jointing pattern best developed to the right of the green patch in the center of the photograph.



Figure 21B. This image is a close-up view of the area on the quarry wall described in Figure 21A. The platy jointing is evident.



Figure 22. Mount McLoughlin with North Squaw Tip prominently displayed form the backdrop for a large hard-rock quarry located in the extreme west-central portion of the Mount McLoughlin quadrangle (see Figure 1), virtually on the boundary with the Willow Lake quadrangle.



Figure 23A. This quarry is located in a lava flow that belongs to the Basaltic Andesite of Dogwood Spring. What makes it attractive as a potential quarry site is the well developed and nearly ubiquitous platy jointing that is so well displayed in this image. It looks very much like an outcrop of the sedimentary rock shale. The platy jointing facilitates breaking the rock into smaller gravel-size fragments.



Figure 23B. What makes this flow and this quarry unusual is the visible presence of the silicate mineral hornblende. Notice in particular the two dark elongate rectangular shaped phenocrysts near the Swiss Army knife; these are euhedral hornblende crystals that are 5 to 8 mm long. The whitish-colored smaller crystals are plagioclase feldspar. This is the solitary location in the Mount McLoughlin quadrangle where hornblende can be found.

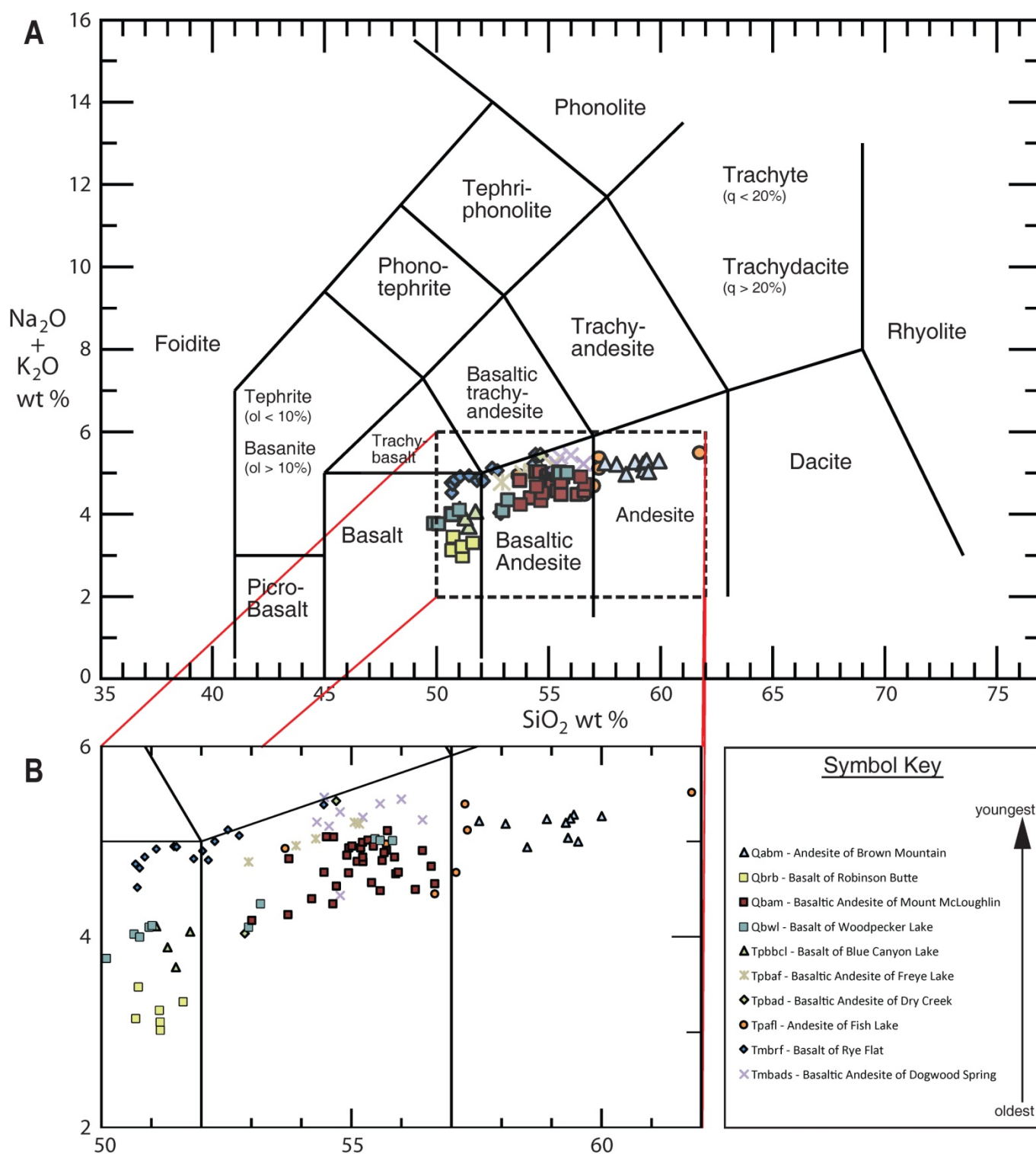


Figure 24. IUGS (International Union of Geological Sciences) classification system for volcanic rocks, which is based on total alkali ($\text{Na}_2\text{O} + \text{K}_2\text{O}$) vs. silica (SiO_2) content, with the superimposed data from analyzed Mount McLoughlin quadrangle samples (including six Qbrb samples from the southwesterly adjacent Robinson Butte quadrangle, plus eleven Qbwl specimens from the easterly adjacent Lake of the Woods North quadrangle; see Table 1) (Le Maitre, 2002).

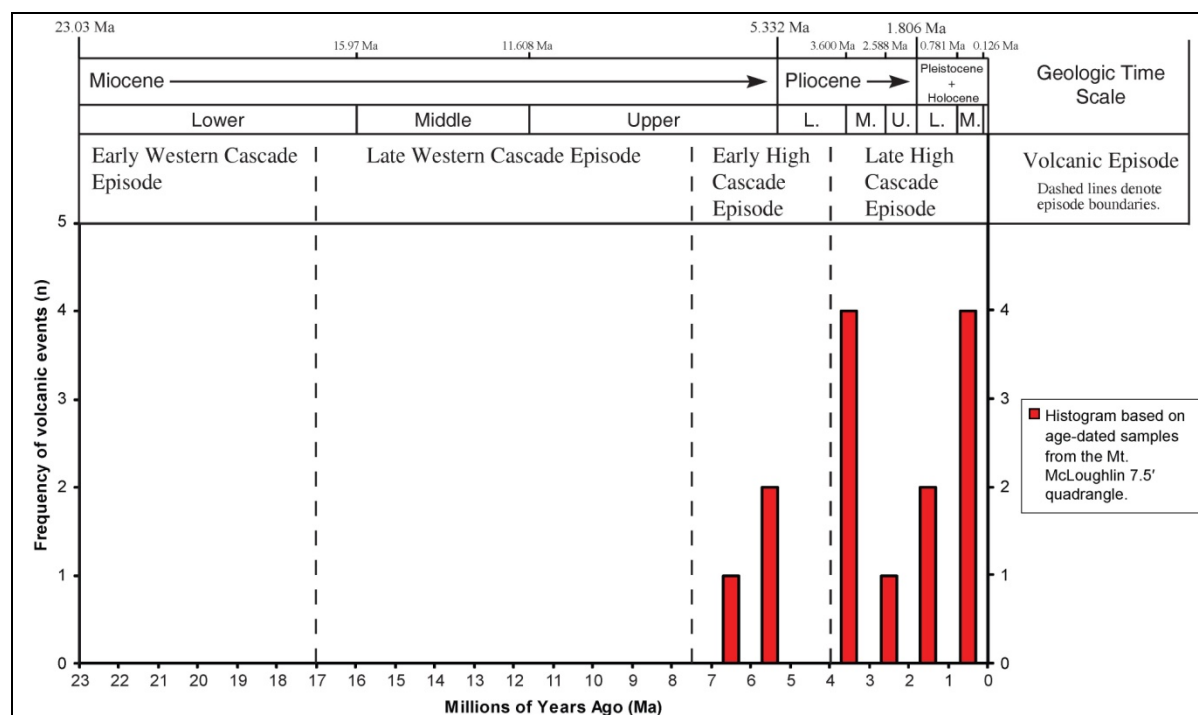


Figure 25A. Histogram (number of samples with either a K-Ar or a $^{40}\text{Ar}/^{39}\text{Ar}$ age plotted as a function of geologic time in millions of years) of the geochronologic data derived from Mount McLoughlin quadrangle samples.

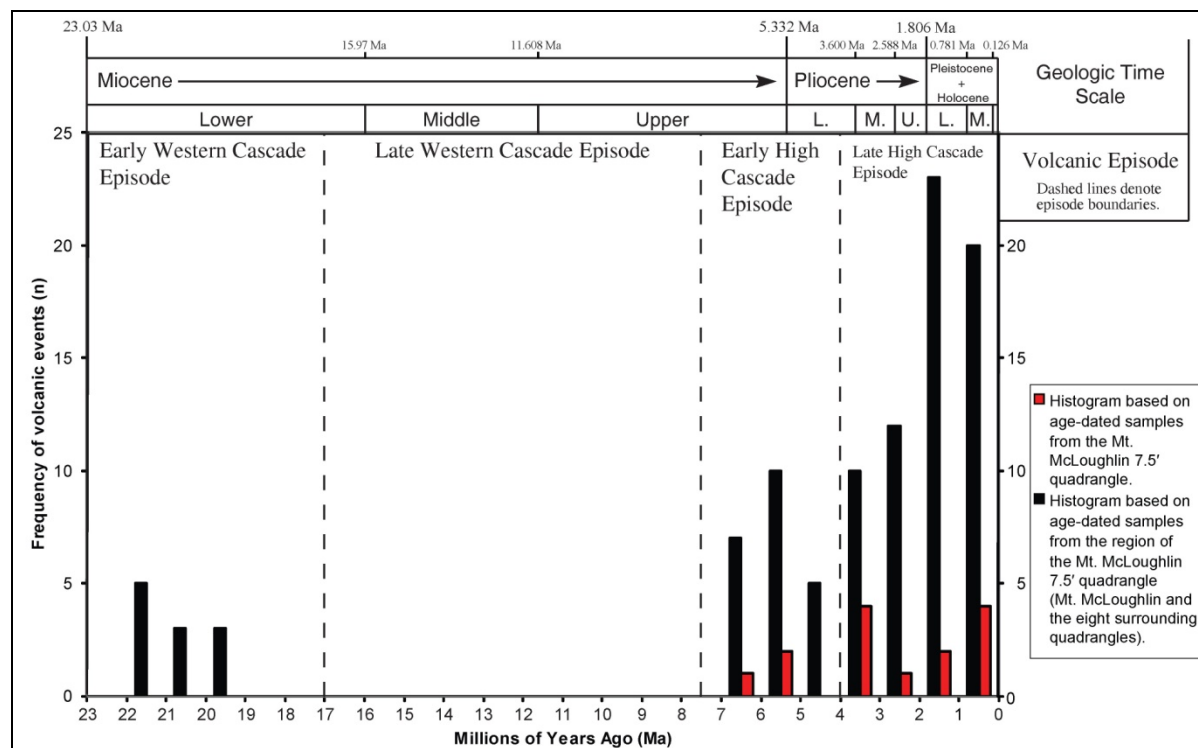


Figure 25B. Histogram of the geochronologic data derived from Mount McLoughlin quadrangle samples plus from samples collected in the eight surrounding quadrangles (see Figure 1).



Figure 26. This image was taken looking down the long axis of Freye Lake, which is located only a few hundred meters off the Pacific Crest Trail east of the summit of Mount McLoughlin. Freye Lake is a glacial lake of natural origin; a number of such lakes dot the northeast corner of the Mount McLoughlin quadrangle.



Figure 27. Viewed from near the Fourmile Lake Dam, the northeast side of Mount McLoughlin appears to have been scooped out and the material deposited as the domelike mass farther to the right in the photograph. This massive landslide has exposed some of the volcano's interior plumbing system as well as the interbedded nature of the flanks of the volcano.



Figure 28A. Hiking the Pacific Crest Trail segment from the cutoff to Mount McLoughlin to Fourmile Lake, one crosses the boundary between the Basaltic Andesite of Freye Lake and the landslide unit. It is a sharp boundary. Large to small angular blocks of lava and pyroclastic material are scattered across the countryside.



Figure 28B. This large block, as big as a pick-up truck, is composed of welded vent agglomerate (Fisher and Schmincke, 1984) with shrinkage cracks clearly evident; it was brought down from high up on the slopes of the volcano.

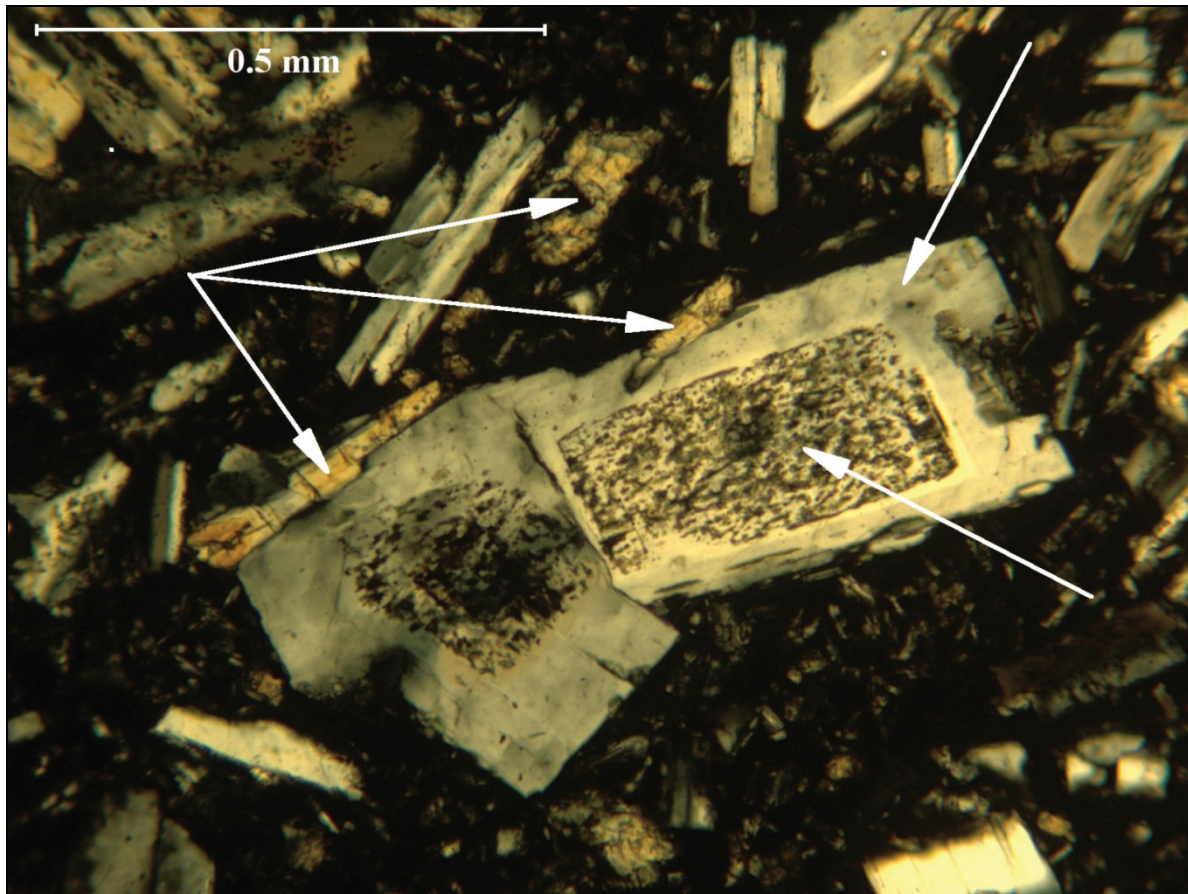
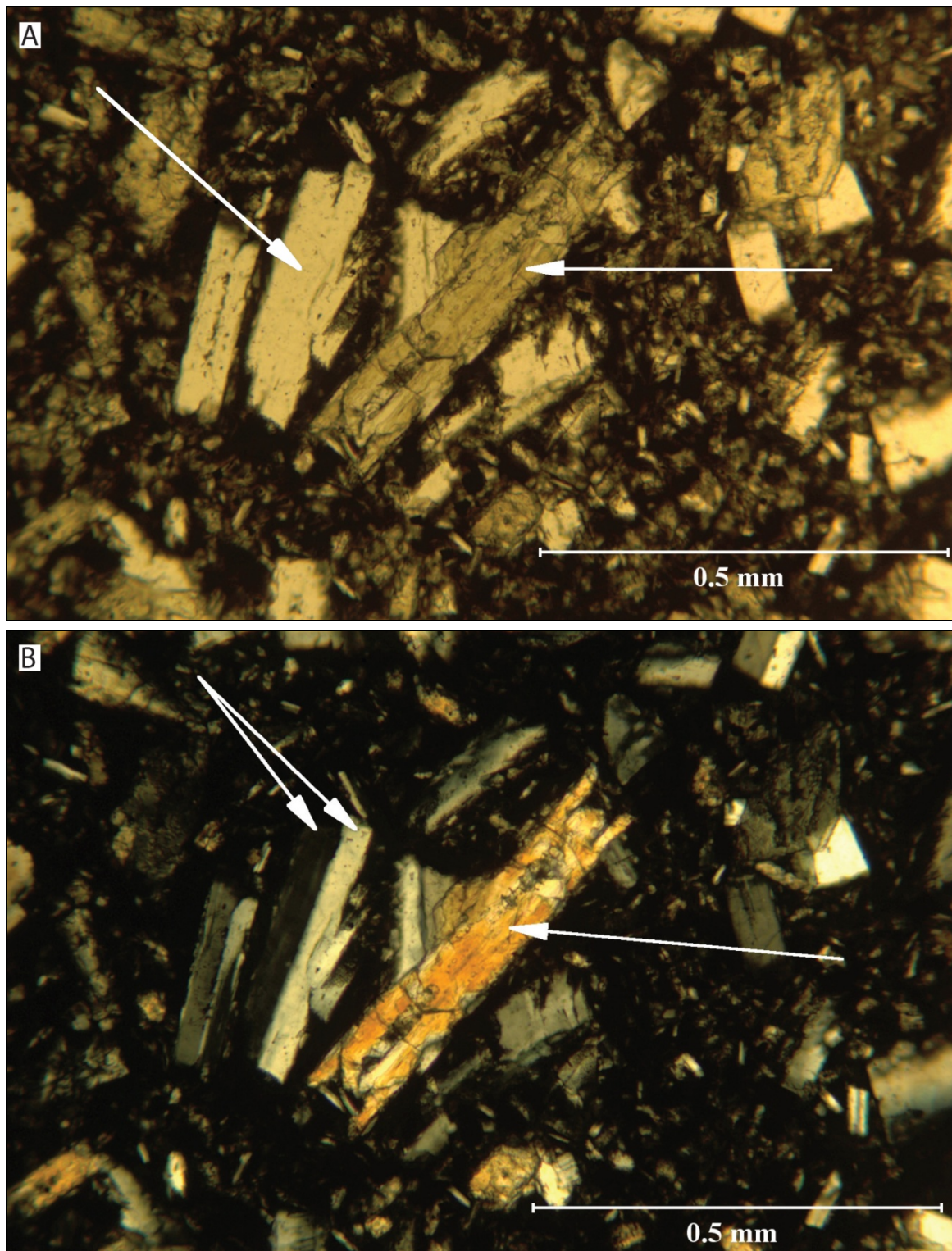
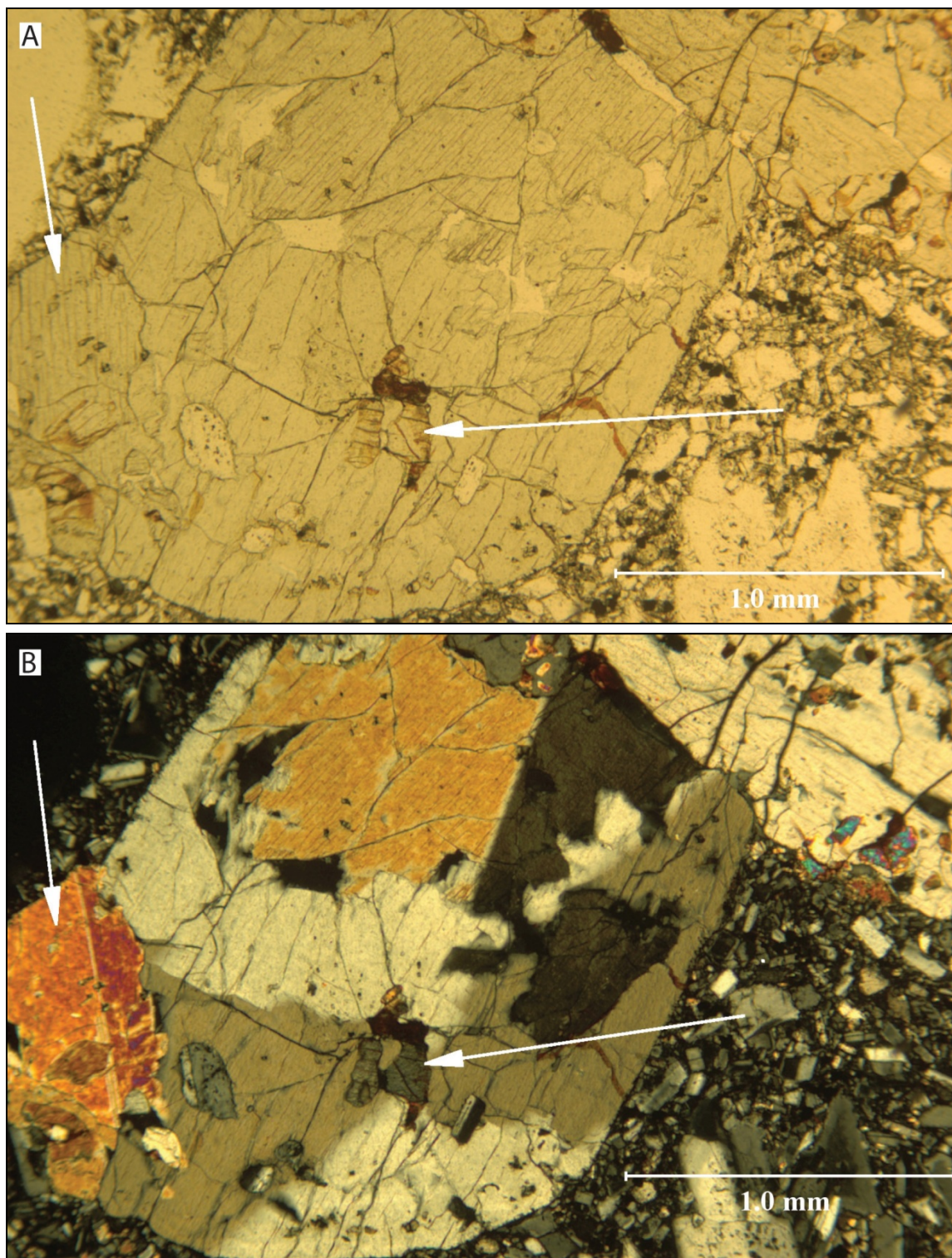


Figure 29. This photomicrograph, taken with crossed polarizers, is from an Andesite of Brown Mountain lava flow. Plagioclase feldspar phenocrysts (two right-hand arrows) invariably contain resorbed cores and clear rims reflecting their magmatic crystallization histories. The left-hand arrows point to orthopyroxene crystals, the most abundant mafic mineral in the Andesite of Brown Mountain.



Figures 30A and 30B. Photomicrograph A, taken with uncrossed polarizers, is also from an Andesite of Brown Mountain lava. The arrow on the left points to a plagioclase crystal, and the other arrow points to an elongate orthopyroxene crystal. In image B, taken with crossed polarizers, the plagioclase crystal is perfectly twinned by the Carlsbad law, while the orthopyroxene crystal depicts imperfect but clearly noticeable sector zoning denoted by the differences in birefringence color.



Figures 31A and 31B. Photomicrograph **A**, taken with uncrossed polarizers, is from a Basaltic Andesite of Mount McLoughlin lava flow depicting a large glomeroporphyritic clump of orthopyroxene, clinopyroxene, and olivine mineral grains. The left-hand arrow points to a pyroxene crystal that has been partially enveloped by the large plate of pyroxene, while the right-hand arrow points to an included olivine grain that has been somewhat altered to iddingsite. In image **B**, taken with crossed polarizers, it becomes apparent that the left-hand arrow marks a twinned clinopyroxene crystal with much higher birefringence than the massive plate of orthopyroxene that has considerably lower birefringence than clinopyroxene. Textural evidence indicates the olivine and clinopyroxene crystallized relatively early in the process and the orthopyroxene crystallized after them.

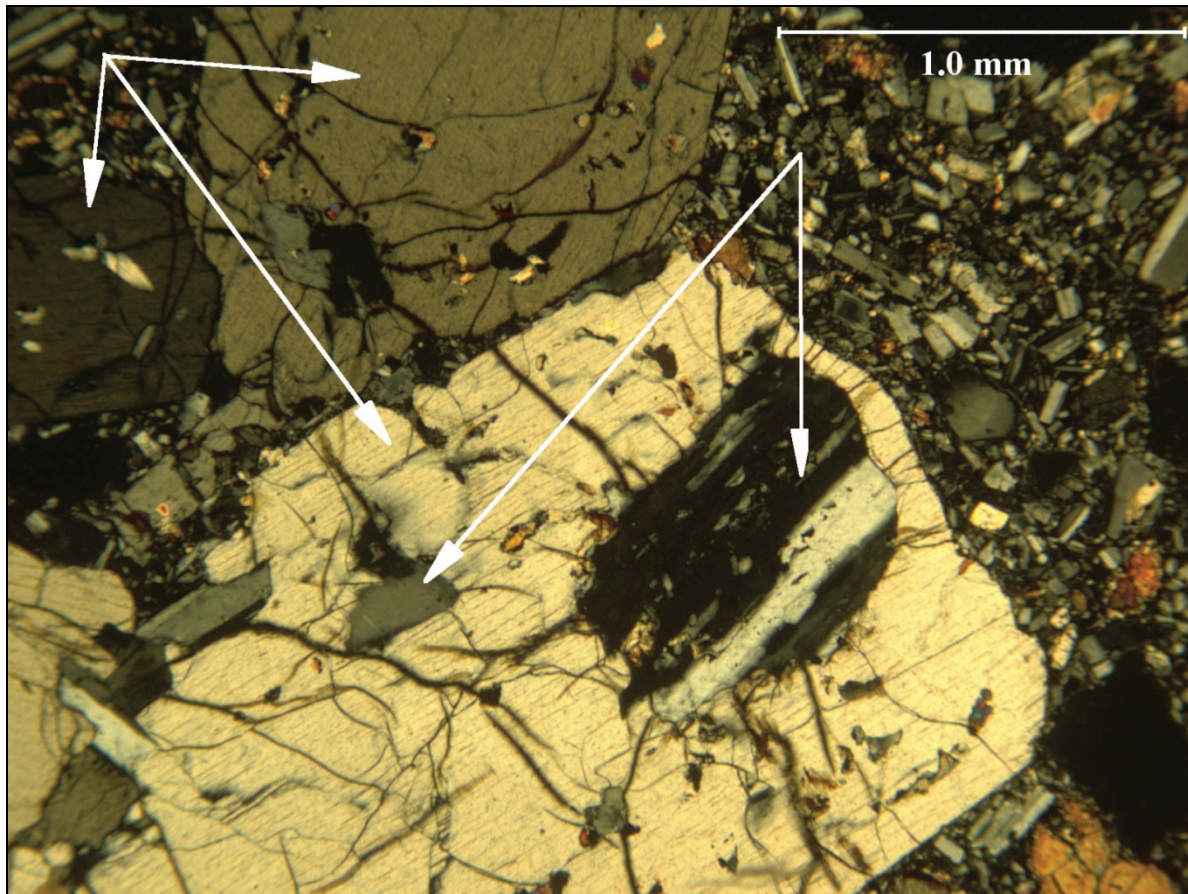
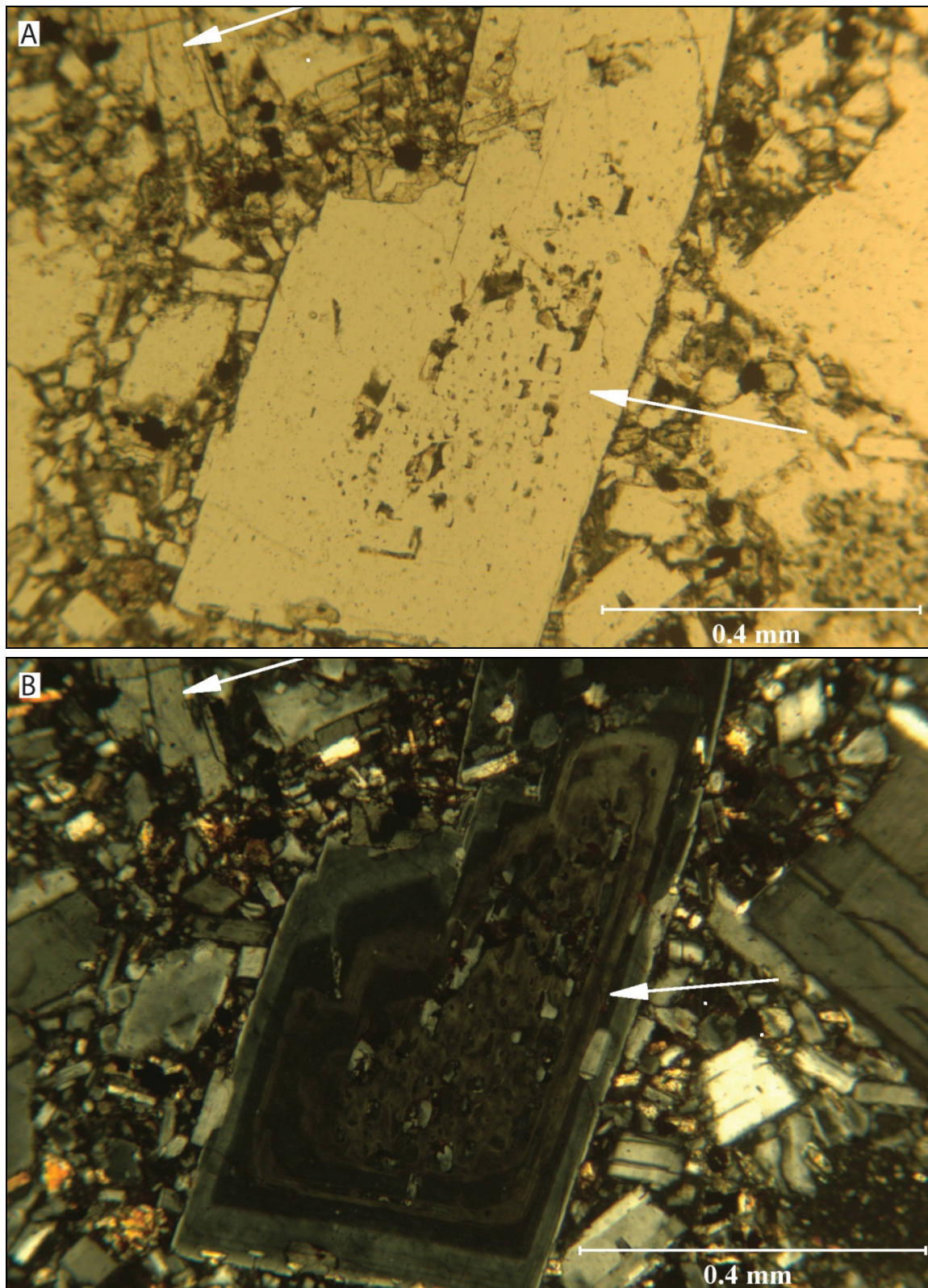
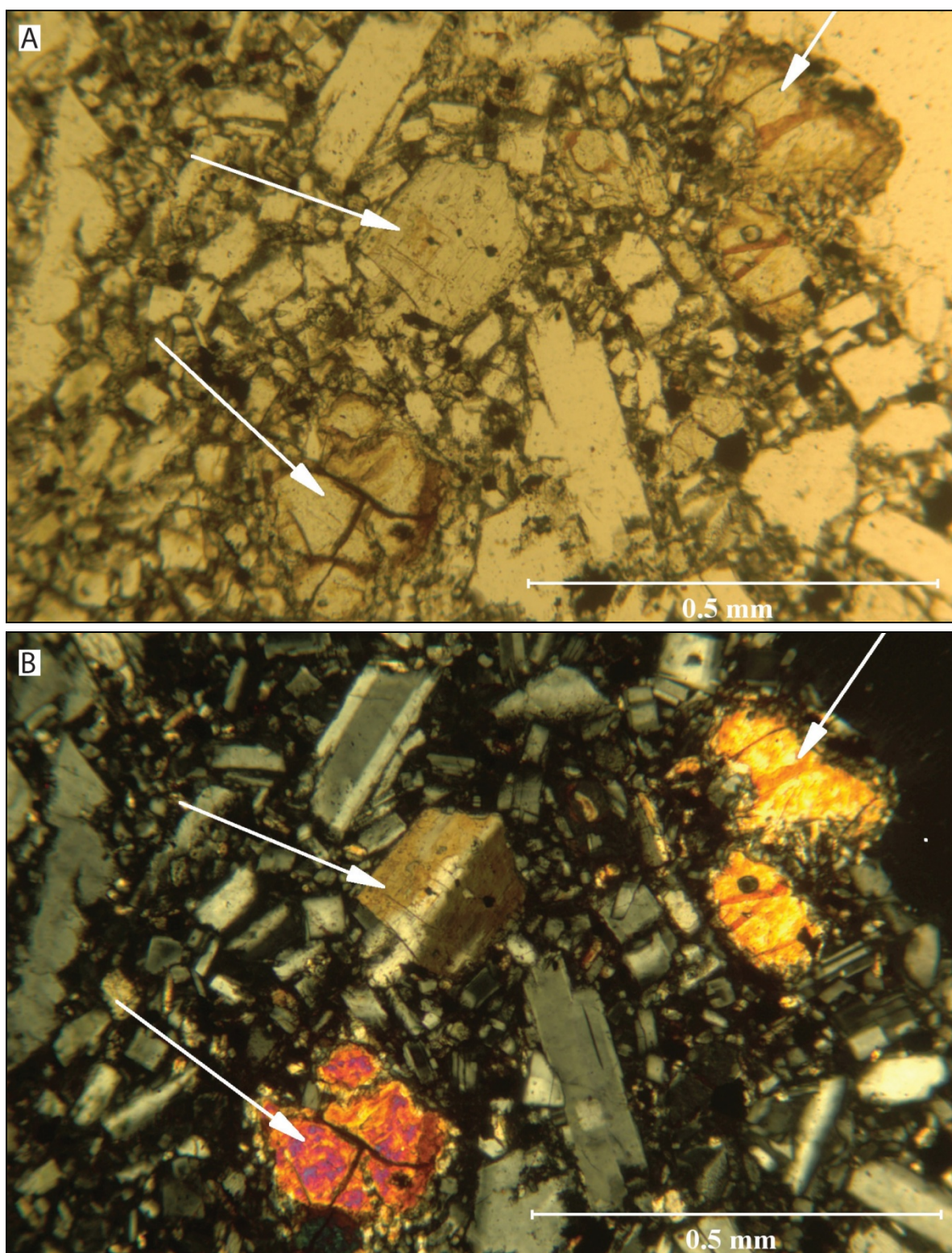


Figure 32. This photomicrograph was taken with crossed polarizers and depicts a large glomeroporphyritic clump that includes three large phenocrysts of low birefringence orthopyroxene (upper-left set of three arrows) that have included within them previously crystallized plagioclase feldspar grains (two right-hand arrows). Taking Figures 31A, 31B, and 32 together strongly suggests that the crystallization sequence for Basaltic Andesite of Mount McLoughlin magma started with olivine, clinopyroxene, and plagioclase, and all three of these minerals were enveloped in large-scale growth of orthopyroxene. What followed after some unknown period of time was movement to the Earth's surface.



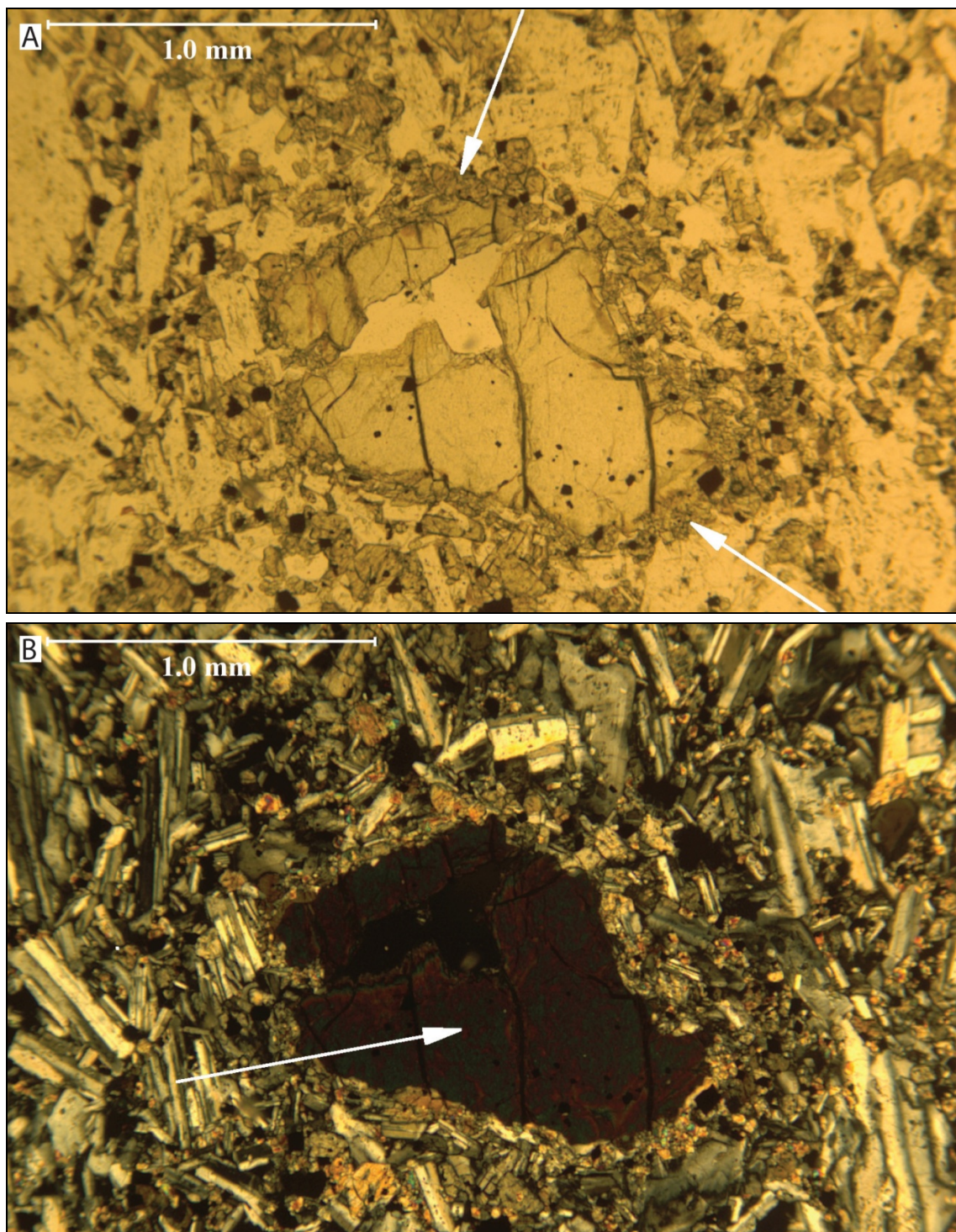
Figures 33A and 33B. Photomicrograph **A**, taken with uncrossed polarizers, depicts a plagioclase feldspar phenocryst whose core region has included blebs of quenched magma and a few small scattered mineral grains (right-hand arrow); such phenocrysts are typical in Basaltic Andesite of Mount McLoughlin lava flows. In image **B**, taken with crossed polarizers, the pattern of chemical zonation within the plagioclase phenocryst is beautifully exhibited.



Figures 34A and 34B. Photomicrograph A, taken with uncrossed polarizers, demonstrates the nature of the matrix that surrounds the phenocrysts present in Basaltic Andesite of Mount McLoughlin lava flows depicted in Figures 31-33. The arrows to the upper-right and lower-left point out olivine crystals, and the arrow in the center marks a clinopyroxene grain together with a large number of variously sized plagioclase crystals. In image B, taken with crossed polarizers, the mineral plagioclase demonstrates that it is more often twinned than not, the euhedral clinopyroxene (center arrow) is twinned as well, and the olivine grains, which have the highest birefringence of all the grains shown, have thin reaction rims of orthopyroxene.



Figure 35. This image is of Smith Rock, which is located in the southeast quarter of the Rustler Peak quadrangle, the one immediately to the north of the Mount McLoughlin quadrangle (see Figure 1). Smith Rock is a volcanic neck, the conduit for an upper Pliocene basalt volcano that is 1.96 ± 0.03 Ma that has been excavated and sculpted by repetitive Pleistocene glaciations.



Figures 36A and 36B. Photomicrograph **A** taken with uncrossed polarizers depicts an olivine phenocryst with a corona of quite small orthopyroxene crystals (see the two arrows). The specific chemical reaction being preserved is: $\text{olivine} + \text{magma} \rightarrow \text{orthopyroxene}$ (see Philpotts, 1989). As basaltic magma slowly crystallizes, the magmatic temperature decreases and can eventually reach the lowest temperature at which olivine crystals and magma can exist together under equilibrium conditions. With further cooling, the chemical reaction between the two phases commences. Note the cubic to rectangular small dark crystals enclosed within the olivine grain (poikilitic texture). These mineral inclusions belong to the spinel-chromite solid solution series and were the first minerals to crystallize from the basaltic magma. In image **B**, taken with crossed polarizers, the arrow is pointing to the olivine crystal, which is nearly at its extinction position, and hence so dark. This orientation makes the corona obvious. The very abundant, gray to white, often rectangular-shaped mineral is plagioclase feldspar.

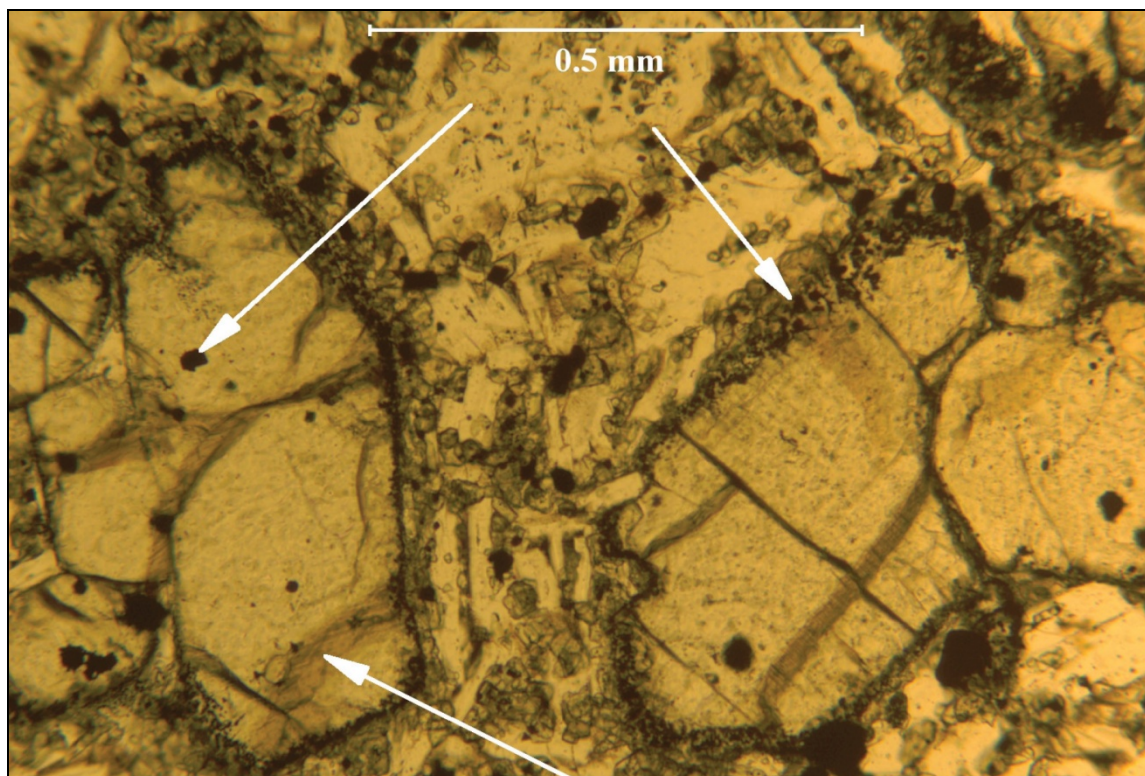


Figure 37. In this photomicrograph, taken with uncrossed polarizers, olivine crystals on the left and right have inclusions of spinel- chromite, an early-formed oxide mineral in the crystallization sequence (see upper-left arrow), while the arrow to the upper-right points to small polygonal-shaped nearly opaque black magnetite (FeFe_2O_4) crystals that form part of a corona structure around the margins of the olivine phenocrysts. This corona is a product of reaction between the hot olivine and a gaseous phase that contains a component of air and was formed in a near-volcanic vent setting. The air component with its abundant O_2 oxidizes the iron in the margins of the olivine crystal from +2 to +3 oxidation state, thus setting the stage for magnetite formation (Haggerty and Baker, 1967). The lower-left arrow is pointing out discoloration along fractures in the olivine that is the result of a much lower temperature alteration of olivine to form iddingsite as a product of both oxidation and hydration chemical reactions (Baker and Haggerty, 1967).



Figure 38. This photograph depicts the typical view of an outcrop of the Basaltic Andesite of Dry Creek. Spheroidal shaped boulders are a manifestation of a combination of chemical and mechanical weathering phenomena. In general there is a correlation between the development of weathering-related characteristics and geologic time assuming that climate has not changed measurably during the time interval between rock formation and observation.

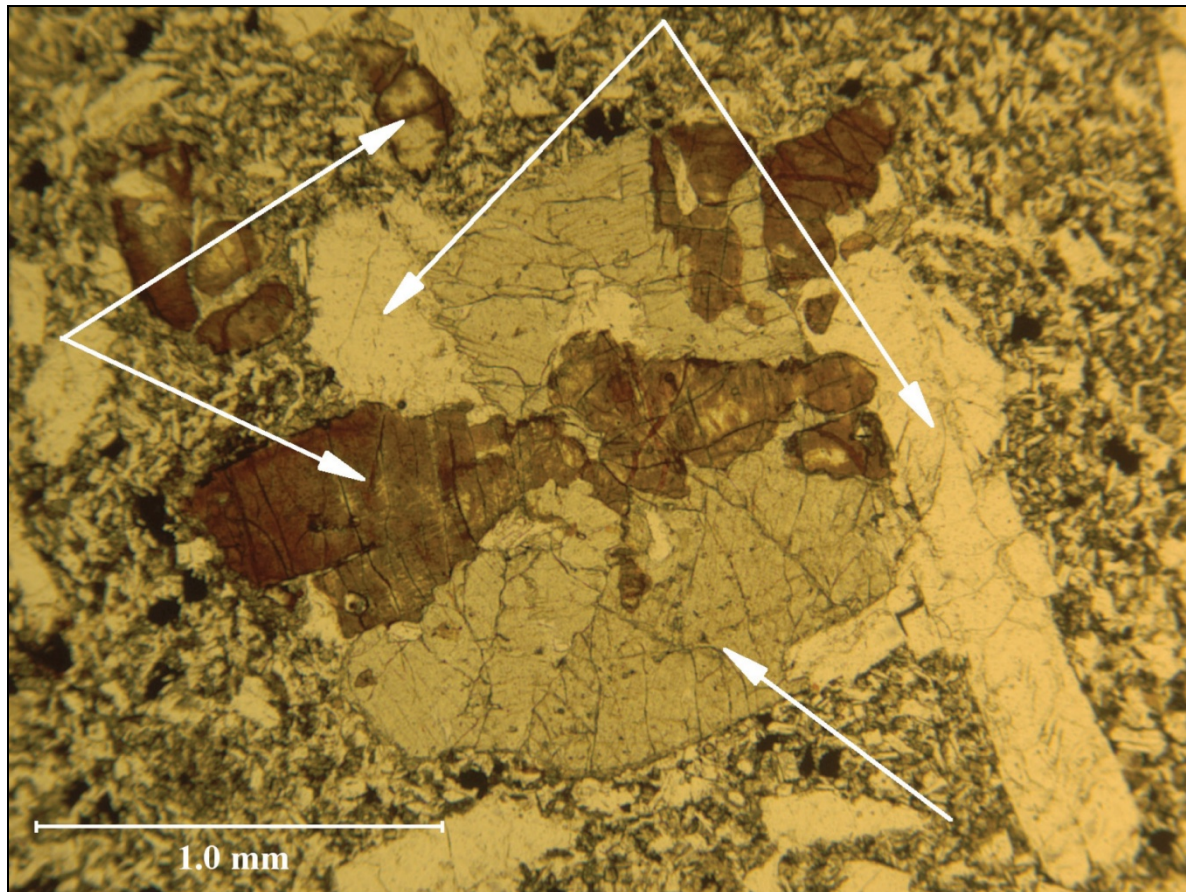
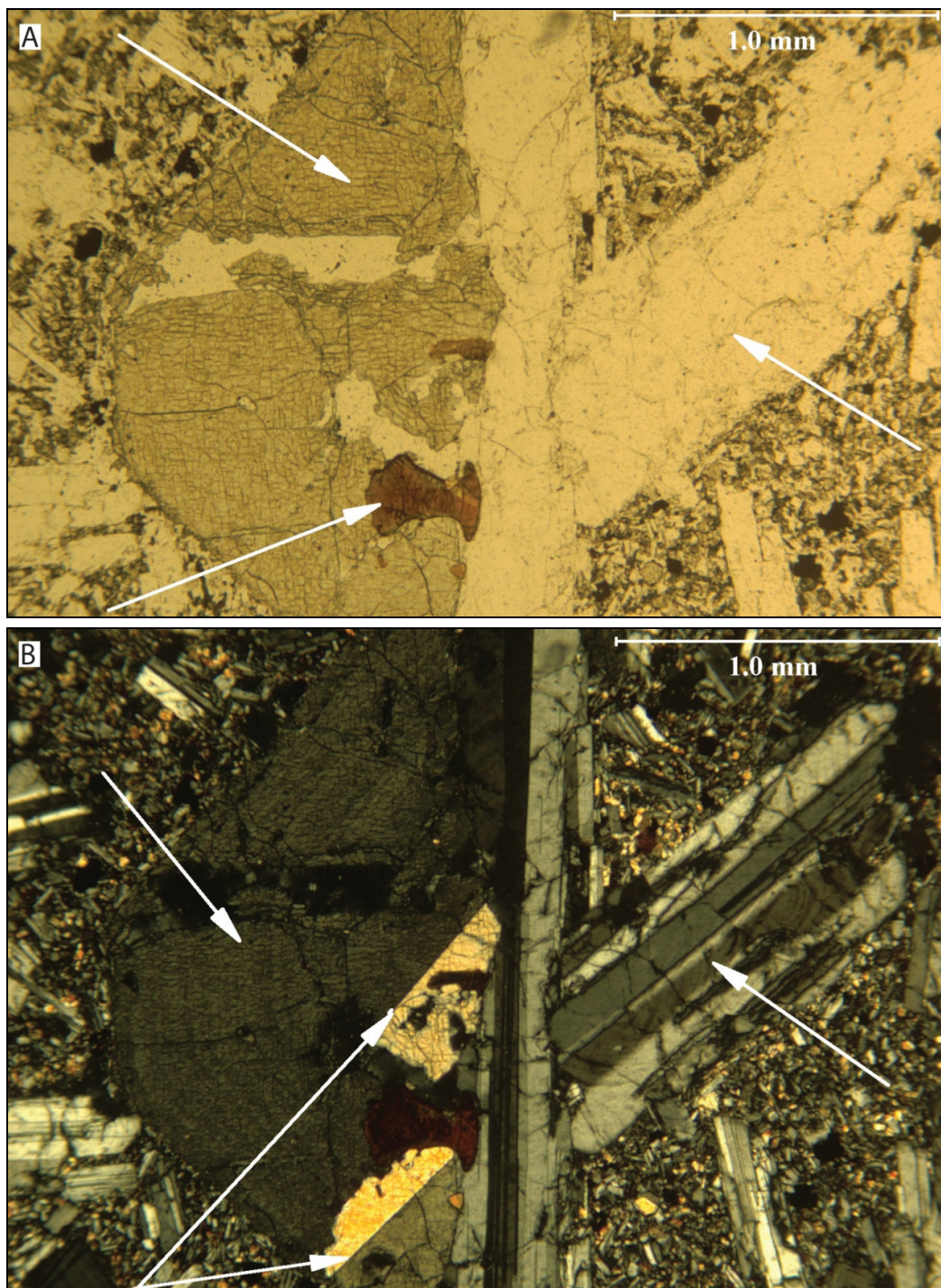


Figure 39. This photomicrograph, taken with uncrossed polarizers, is from a Basaltic Andesite of Dry Creek lava flow. In the large glomeroporphyritic clump shown, the leftmost two arrows point to olivine phenocrysts that have suffered substantial alteration to iddingsite, the upper two arrows point to plagioclase feldspar phenocrysts, and the singular arrow points to a large grain of clinopyroxene that is encompassing several olivine grains. Thus, in terms of crystallization history the Basalt of Pearce Point and the Basaltic Andesite of Dry Creek have much in common.



Figures 40A and 40B. Photomicrograph A, taken with the polarizers uncrossed, is from a Basaltic Andesite of Dry Creek lava flow. The upper left-hand arrow points out a large clinopyroxene phenocryst with well-developed cleavage that surrounds a much smaller olivine crystal that has been substantially altered to iddingsite (lower left-hand arrow), while the right-hand arrow points to one of two large plagioclase phenocrysts, thus forming a glomeroporphyritic clump. In image B, taken with crossed polarizers, the left-hand arrow marks well-developed but subtle oscillatory zoning in the clinopyroxene phenocryst while the two bottommost arrows point to two clinopyroxene grains not obvious in the previous image that are quite nicely twinned by the Carlsbad law. The right-hand arrow points out a complexly twinned plagioclase feldspar, twinned by the Albite law, while both the Carlsbad as well as the Albite law twin other crystals.

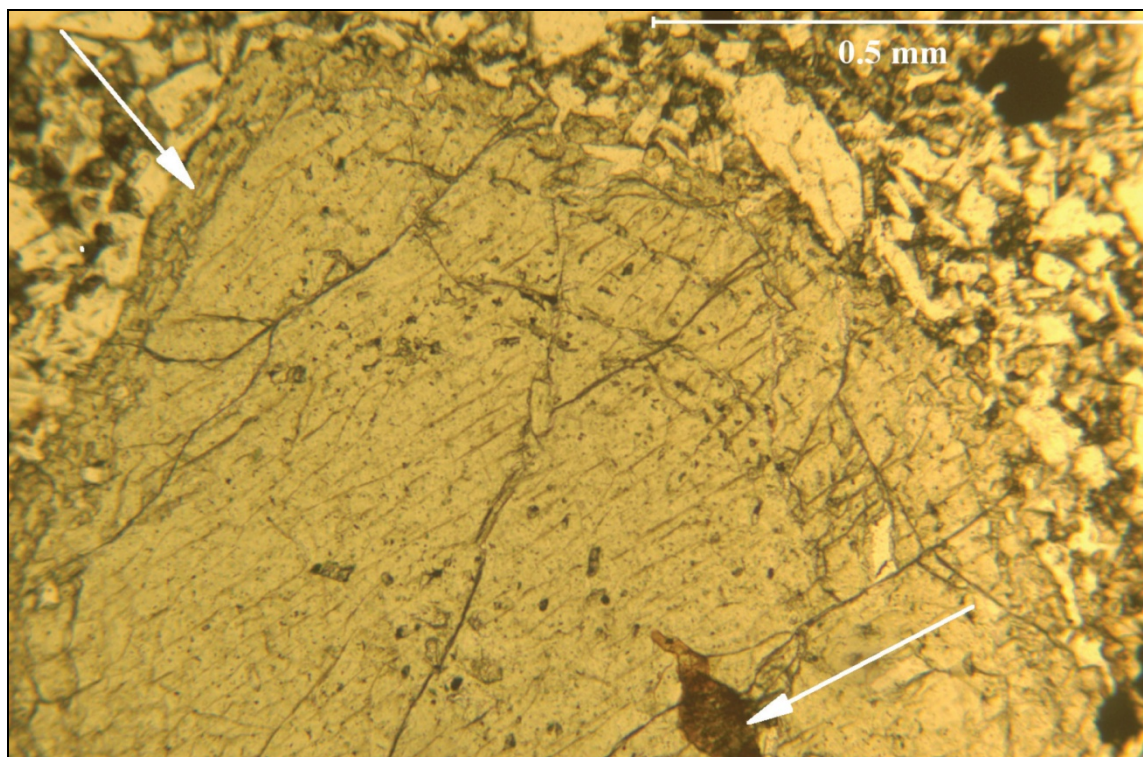


Figure 41. This photomicrograph, taken with uncrossed polarizers, is from a Basaltic Andesite of Dry Creek lava flow. The top-left arrow points to the margin of a large clinopyroxene phenocryst that has been resorbed to a degree on its periphery, somehow affected by changing physical conditions in the magma. The lower arrow points to an included olivine crystal that has been totally converted to iddingsite. To a certain extent the larger phenocryst minerals act as memory devices recording the changes in physical environment through compositional and textural changes.



Figure 42. This image was taken from the Pacific Crest Trail as it rounds Brown Mountain on its northeast side. To the right is Mount McLoughlin and to the left the low-profile hump is the Rye Flat shield volcano with a capping of Basaltic Andesite of Dogwood Spring (see geologic map). Today the remnants of the Basalt of Rye Flat are exposed to the west and southwest of the volcano. In all other directions the Basalt of Rye Flat is covered by younger volcanic rock.



Figure 43. Driving east from Medford to Klamath Falls, Oregon, on state highway 140, two miles before 1) the turnoff to the south on USFS road 37 or 2) the turnoff to the north onto Jackson County 821 to Butte Falls, massive 20 to 25 m thick outcrops of Basalt of Rye Flat are encountered.



Figure 44. At the same locale described in Figure 43, Basalt of Rye Flat also crops out in columnar-jointed lava flows, the cross-sectional morphology of which makes one think of a channel-filling lava flow.



Figure 45A. At the same locale described in Figure 43, particularly on the far right-side of the image, you can see joint planes that curve up to the right, defining the channel margin.



Figure 45B. Interspersed with lava flows that vary in morphology from quite massive to columnar jointed are relatively thick layers of partially lithified pyroclastic material that varies in size from ash to bombs (Fisher and Schmincke, 1984). This material is Basalt of Rye Flat.

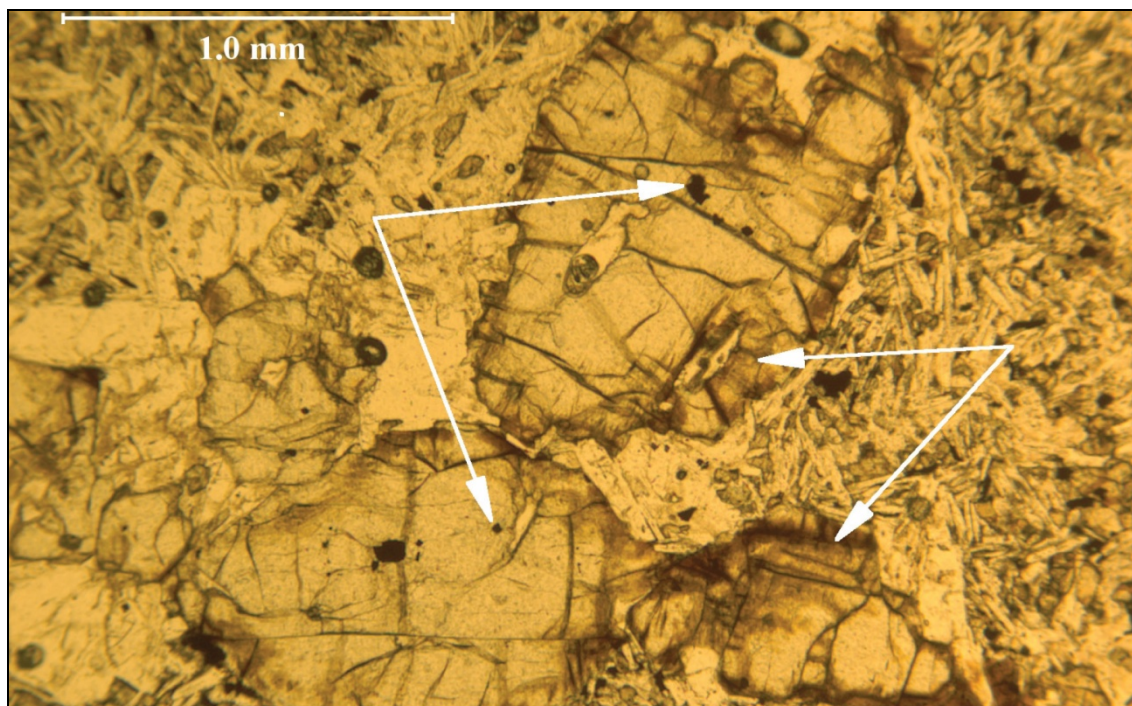


Figure 46A. In this photomicrograph, taken with uncrossed polarizers, a glomeroporphyritic clump of olivine phenocrysts is depicted. The left-hand arrows point to poikilitically enclosed early-formed spinel crystals, and the right-hand two arrows point to patches of low-temperature alteration to iddingsite (Baker and Haggerty, 1967). This texture is typical of Basalt of Rye Flat.

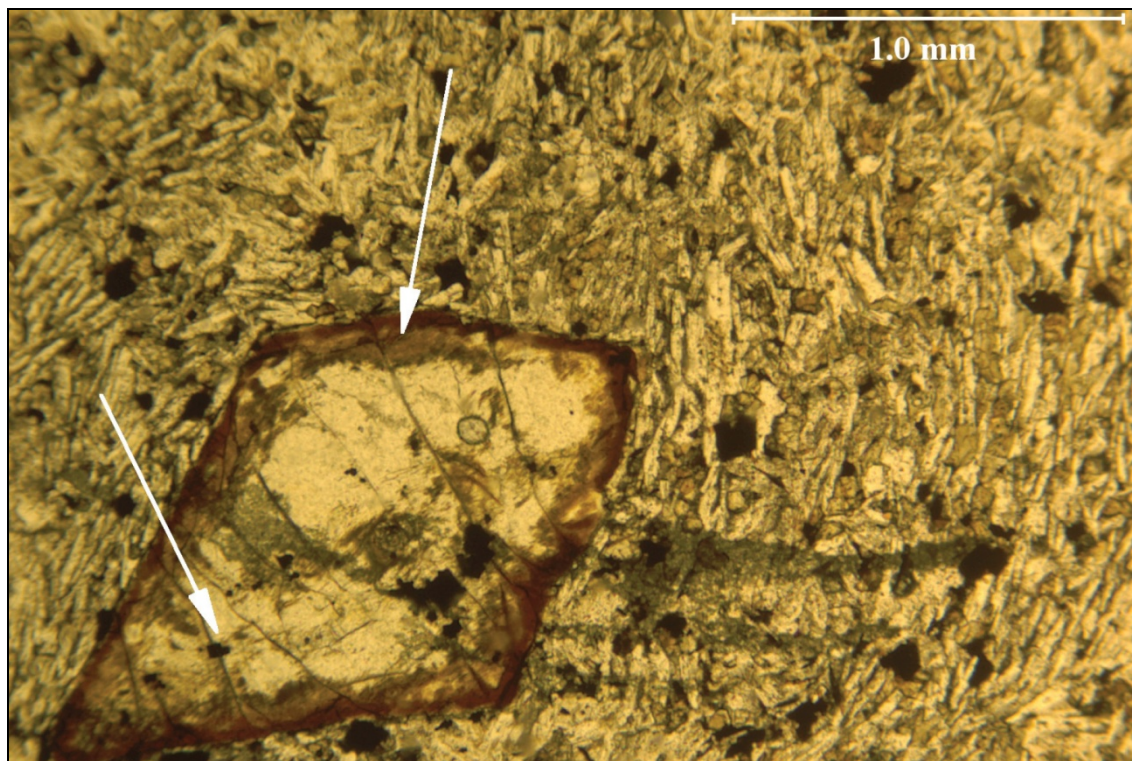


Figure 46B. This photomicrograph taken with uncrossed polarizers shows two features. The swirling pattern of light-colored rectangular-shaped plagioclase crystals and darker colored but similar-sized pyroxene crystals is the result of lava flowage. The large olivine grain is an island in the stream. The resulting texture is known as trachytic (Philpotts, 1989). Second, the lower left-hand arrow points to a spinel crystal that was engulfed by the growing olivine at the time of crystallization, while the upper right-hand arrow points to intense marginal alteration to iddingsite. The alteration to iddingsite commonly follows fractures in an olivine crystal.



Figure 47A. Basaltic Andesite of Dogwood Spring lava flows often are the victims of intense spheroidal weathering. The geometric shape of the outcrop suggests this lava flow filled a preexisting stream channel on the surface of the Earth as the lava was flowing away from its vent.



Figure 47B. Basaltic Andesite of Dogwood Spring lava flows often have well-developed platy jointing formed during the cooling process at the Earth's surface. Individual plates are between 8 and 12 cm thick.

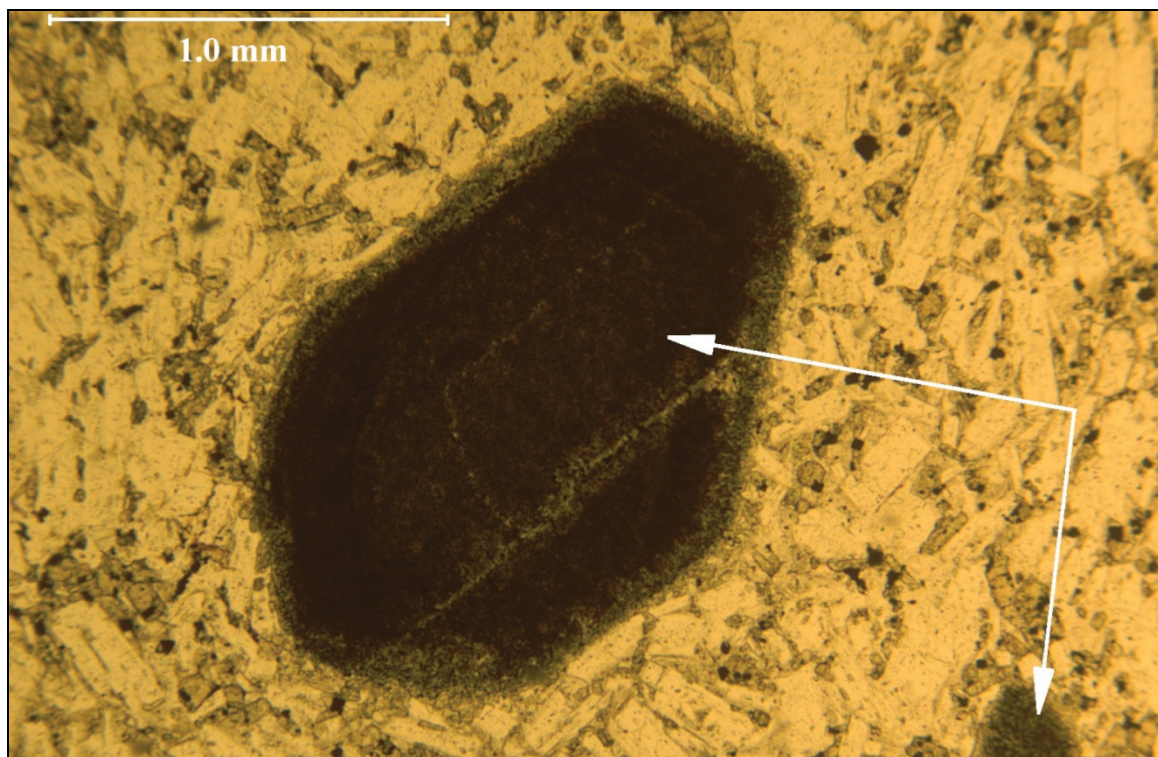


Figure 48. In this photomicrograph, taken with uncrossed polarizers, a euhedral pseudomorph of an amphibole phenocryst is beautifully preserved. The six-sided crystal shape and the angular relationships between the six sides (faces) are indicative of amphibole.

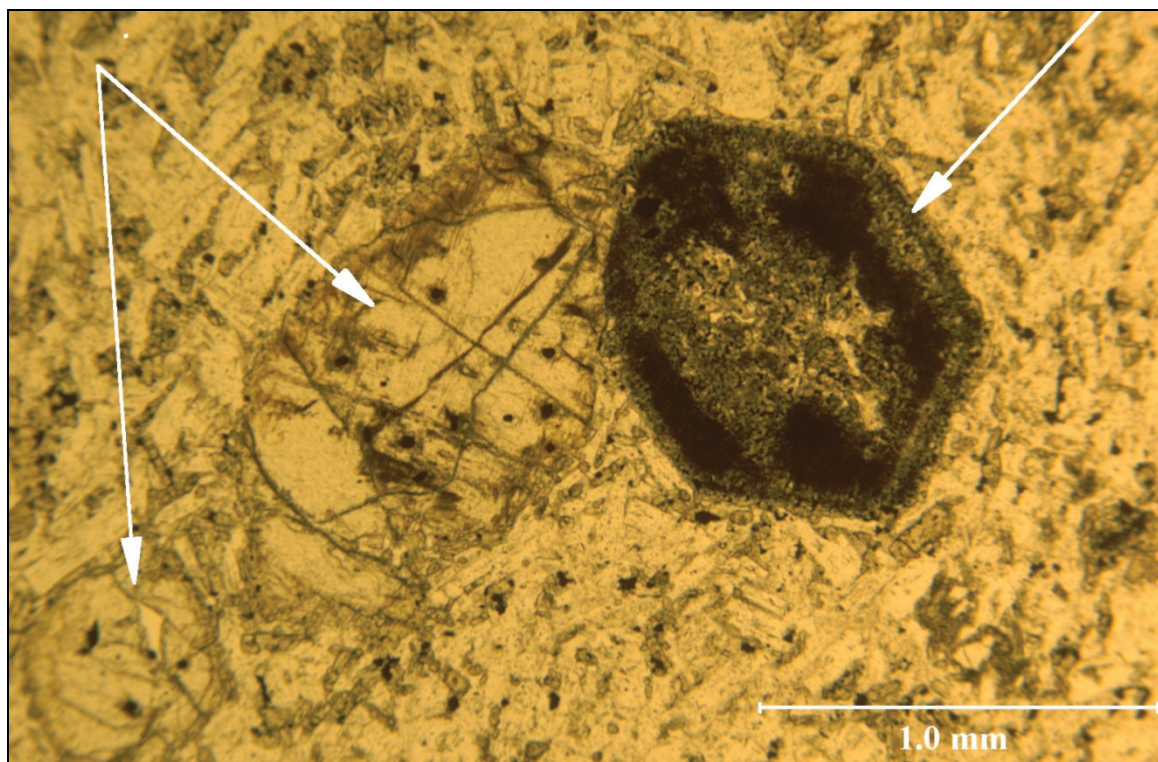


Figure 49. This photomicrograph, taken with the polarizers uncrossed, demonstrates the co-existence of olivine on the left with inclusions of spinel and some marginal alteration to iddingsite closely juxtaposed to a euhedral pseudomorph of amphibole. The amphibole, which most likely was hornblende in composition, broke down during the extrusion process as the water pressure (P_{H_2O}) decreased to zero (see text for a more complete explanation).

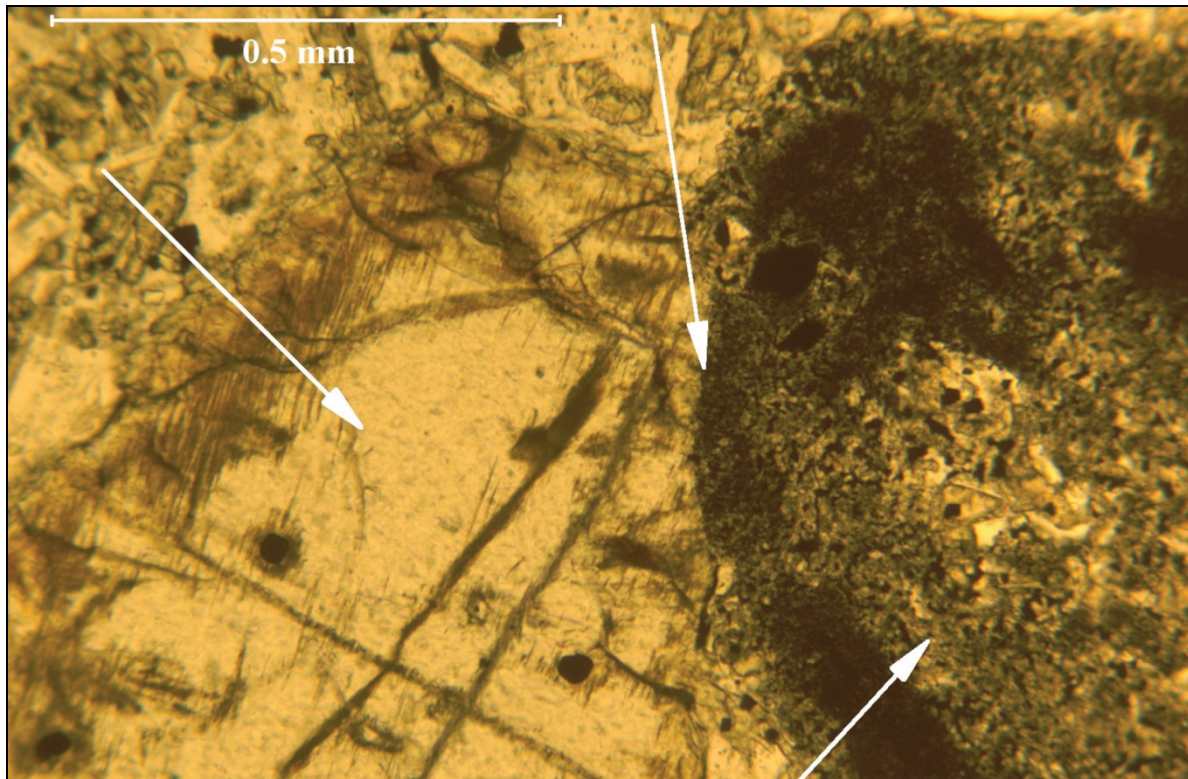


Figure 50. The goal of this photomicrograph, taken under uncrossed polarizers, is to demonstrate “textural equilibrium,” that is, where two mineral grains are actually in contact with one another and thus suggest the minerals constitute an equilibrium assemblage. Olivine is on the left-hand side, the hornblende pseudomorph is on the right-hand side, and the central arrow points to where the two minerals are definitely touching.

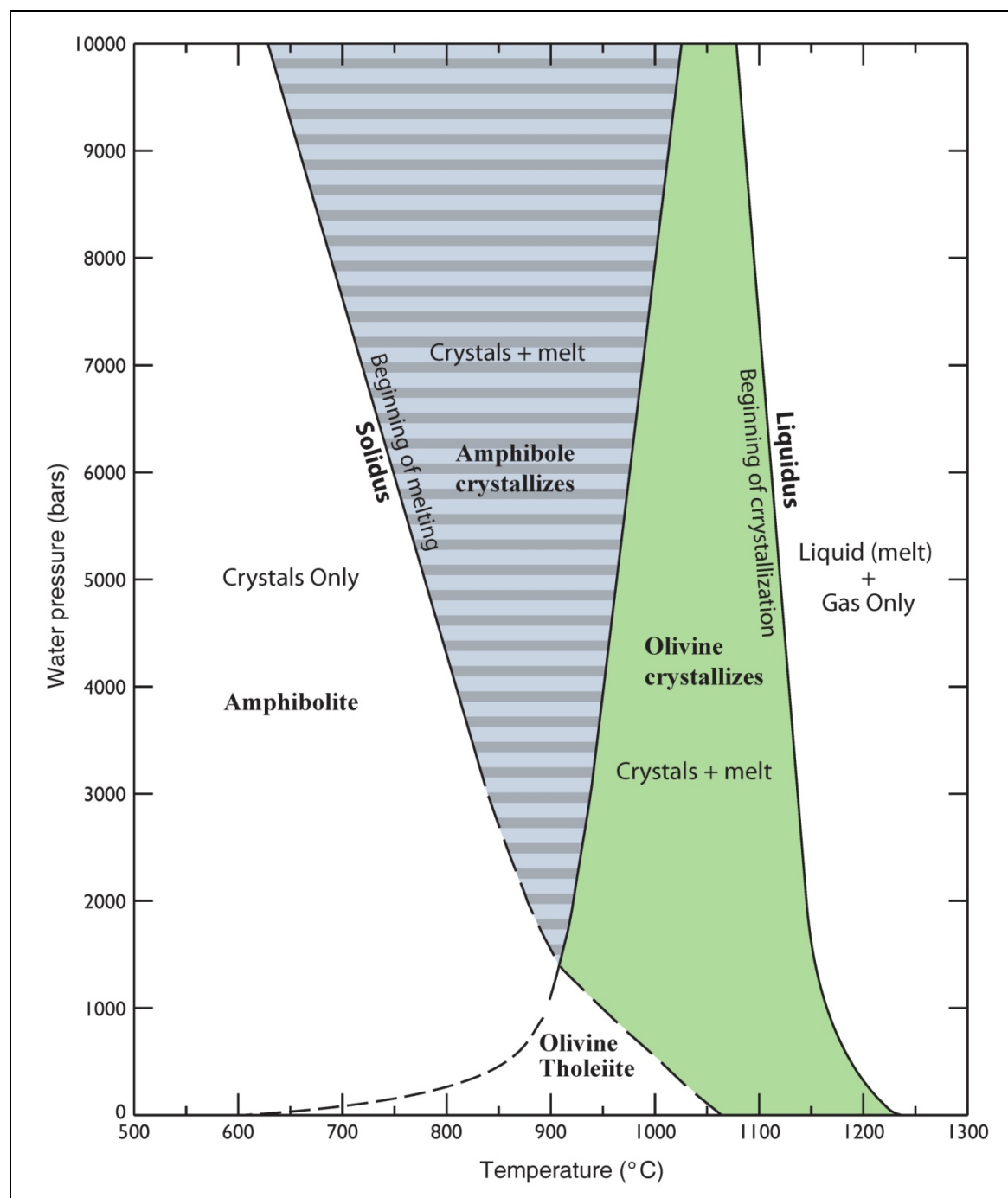


Figure 51. In this pressure versus temperature sketch it is important to note that the pressure is water pressure (P_{H_2O}) and not just load pressure (for example, see Eggler, 1972; Yoder and Tilley, 1962). Thus, a hydrous mineral like amphibole will be stable in such a system. However, when the pressure is released, hydrous minerals will rapidly become unstable and react. Notice the curves representing olivine and amphibole stability cross in the neighborhood of 12,000 bars water pressure. That is at a depth of approximately 40 km. The textural relationships preserved in this one Basaltic Andesite of Dogwood Spring lava flow suggest the original magma began its ascent to the surface from a depth of nearly 40 km and did so rather rapidly given the well-preserved state of the amphibole pseudomorphs (Rutherford, 2008).

Table 1 (page 1). Whole rock chemical data and potassium-argon (K-Ar) ages (^a indicates an argon-argon age) for the samples from the Preliminary Geologic Map of the Mt. McLoughlin 7.5' Quadrangle, Jackson and Klamath Counties, Oregon. The major element oxides are presented in weight percent and the trace elements are reported in parts per million (ppm). The chemical data are X-ray fluorescence (XRF) results and were measured in the X-ray laboratory of the Department of Earth and Environment, Franklin and Marshall College, Lancaster, Pennsylvania. The UTM coordinate values are according to the UTM Zone 10 (NAD 27 for US) projection. All UTM coordinates have been rounded to the nearest 10 m. The 1/4 of 1/4, Section (Sec.), Township (T.), and Range (R.) columns are location descriptors of the Public Land Survey System (PLSS) (Willamette meridian and base line). In the Lithology column (Lith.), B = basalt (SiO₂ = 45-52%), BA = basaltic andesite (SiO₂ = 52-57%), A = andesite (SiO₂ = 57-63%), BTra = basaltic trachyandesite (consult Figure 24 of this report). See Figure 24 and Le Maitre (2002) for details regarding lithological classification. Please consult the detailed descriptions in this report or the geologic map for the full unit names. This table is 2 pages long.

Map	Sample	K-Ar Age ^a (Ma)	1/4	1/4 Sec.	T.	UTM N	Unit	Lith.	SiO ₂	TiO ₂	Al ₂ O ₃	Fe ₂ O ₃	FeO	MnO	MgO	CaO	Na ₂ O	K ₂ O	P ₂ O ₅	LOI	Total	Fe ₂ O ₃ T	Rb	Sr	Y	Zr	V	Ni	Cr	Nb	Ga	Cu	Zn	Co	Ba	La	Ce	U	Th	Sc	Pb	Yb	Be			
1	84-21	5.97 ± 0.36	SW	SE	27	36	4	554870	4894960	Tmbas	BTra	54.45	1.06	18.31	2.91	5.21	0.14	3.81	7.69	4.24	1.21	0.51	0.63	100.17	8.70	11.7	840	24.4	114	156	10	32	7.4	23.3	60	65	24	526	20	42	0.7	3.8	17	6	1.7	1.7
2	M91-85A	6.43 ± 0.10	NW	SW	16	36	4	552540	4896250	Tmbas	BA	56.00	1.02	17.92	3.30	4.50	0.12	3.68	7.01	3.97	1.46	0.51	0.88	100.37	8.30	13.2	931	23.1	123	158	16.4	50	8.2	23.3	60	65	24	528	20	42	0.7	3.8	17	6	1.7	1.7
3	91-89	5.62 ± 0.09	NW	SE	20	36	4	551530	4897060	Tmbas	BA	56.41	1.00	18.11	2.95	3.87	0.10	4.02	6.99	4.05	1.17	0.26	1.27	100.01	7.25	9.7	861	16.1	74	163	27	89	4.1	22.9	148	63	22	344	10	23	3.4	1.3	4.6	17	0.9	1.4
4	04SM-5	—	NW	SE	17	36	4	554680	4895100	Tmbas	BA	54.31	1.06	18.12	2.77	5.24	0.15	3.84	7.07	3.97	1.22	0.52	0.63	99.71	8.97	15	853	23	129	169	20	24	7.4	21.6	373	72	22	566	—	—	0.5	2	19	6	—	—
5	H91-48	—	NW	SE	34	36	4	554700	4894560	Tmbas	BA	54.95	1.12	17.18	2.85	5.51	0.15	4.03	6.91	3.93	1.22	0.52	0.63	99.71	8.97	15	853	23	129	169	20	24	7.4	21.6	373	72	22	566	—	—	0.5	2	19	6	—	—
6	M91-81E	—	NW	SE	16	36	4	552930	4896430	Tmbas	BA	54.75	1.04	18.46	2.72	4.38	0.14	3.80	7.06	3.99	1.31	0.52	0.99	100.44	8.59	12	860	25	132	159	31	72	—	—	26	457	20	36	—	—	21	—	1.6	1.9	—	—
7	M91-98	—	NW	SE	21	36	4	552520	4897770	Tmbas	BA	54.73	0.78	18.75	2.75	4.12	0.12	4.12	7.17	4.11	1.13	0.28	1.25	99.87	7.33	9.2	880	12	113	168	38	62	3.8	21.5	162	60	17	363	12	23	-0.5	1.7	1.7	—	—	
8	09SM-36	—	NW	SE	16	36	4	551330	4897070	Tmbas	BA	55.58	1.01	17.54	3.45	4.06	0.14	3.50	7.14	3.92	1.46	0.51	1.11	99.42	7.96	14.4	940	22.6	137	137	25	22	7.4	21.2	58	75	20	723	—	-0.5	2	15	5	—	—	
9	09SM-35	—	NW	SE	16	36	4	552660	4897950	Tmbas	BA	56.07	1.18	17.29	3.34	6.27	0.17	3.58	8.04	3.64	1.13	0.50	1.51	100.12	10.31	11.1	885	34.2	144	202	82	121	7.3	21.3	101	85	30	528	20	41	-0.5	2.1	24	2	—	—
10	09SM-34	—	NW	SE	34	36	4	555400	4892560	Tmbas	B	50.74	1.20	17.32	4.04	5.66	0.17	5.29	8.36	3.58	0.95	0.57	1.18	100.47	10.83	7	862	31	136	226	54	91	—	—	38	453	24	44	—	—	23	—	2.4	1.9	—	—
11	H91-41	—	NW	SE	5	37	4	551880	4892560	Tmbas	B	50.74	1.20	17.32	4.04	5.66	0.17	5.29	8.36	3.58	0.95	0.57	1.18	100.47	10.83	7	862	31	136	226	54	91	—	—	38	453	24	44	—	—	23	—	2.4	1.9	—	—
12	09SM-34	—	NW	SE	5	37	4	551880	4892560	Tmbas	B	50.74	1.20	17.32	4.04	5.66	0.17	5.29	8.36	3.58	0.95	0.57	1.18	100.47	10.83	7	862	31	136	226	54	91	—	—	38	453	24	44	—	—	23	—	2.4	1.9	—	—
13	09SM-31	—	NW	SE	5	37	4	551640	4892560	Tmbas	B	50.84	1.19	17.40	3.67	5.80	0.17	6.04	8.28	3.72	1.11	0.51	1.05	100.00	10.12	9.2	969	20.8	139	230	78	207	6.7	21	95	84	29	556	16	40	-0.5	0.8	20	2	—	—
14	09SM-31	—	NW	SE	5	37	4	551640	4892560	Tmbas	B	50.84	1.19	17.40	3.67	5.80	0.17	6.04	8.28	3.72	1.11	0.51	1.05	100.00	10.12	9.2	969	20.8	139	230	78	207	6.7	21	95	84	29	556	16	40	-0.5	0.8	20	2	—	—
15	M91-44	—	NW	SE	28	36	4	552300	4895070	Tmbas	B	51.43	1.25	17.97	3.26	6.38	0.17	5.05	8.44	3.74	1.20	0.57	1.01	100.27	10.35	8	849	35	135	215	44	102	—	—	33	537	23	45	—	—	23	—	2.7	1.7	—	—
16	09SM-37	—	NW	SE	28	36	4	552300	4895070	Tmbas	B	51.43	1.25	17.97	3.26	6.38	0.17	5.05	8.44	3.74	1.20	0.57	1.01	100.27	10.35	8	849	35	135	215	44	102	—	—	33	537	23	45	—	—	23	—	2.7	1.7	—	—
17	H91-42	—	NW	SE	34	36	4	554540	4893260	Tmbas	B	51.83	1.30	18.04	3.32	6.16	0.17	4.81	8.06	3.81	1.01	0.60	1.54	100.59	10.17	11	850	35	135	204	40	74	—	—	36	503	32	45	—	—	23	—	2.7	1.9	—	—
18	H91-43	—	NW	SE	34	36	4	554540	4893260	Tmbas	B	51.83	1.30	18.04	3.32	6.16	0.17	4.81	8.06	3.81	1.01	0.60	1.54	100.59	10.17	11	850	35	135	204	40	74	—	—	36	503	32	45	—	—	23	—	2.7	1.9	—	—
19	H91-44	—	NW	SE	34	36	4	554540	4893260	Tmbas	B	51.83	1.30	18.04	3.32	6.16	0.17	4.81	8.06	3.81	1.01	0.60	1.54	100.59	10.17	11	850	35	135	204	40	74	—	—	36	503	32	45	—	—	23	—	2.7	1.9	—	—
20	M91-31	—	SE	SE	32	36	4	552070	4893260	Tmbas	BA	52.01	1.17	17.46	4.22	5.11	0.16	4.99	8.05	3.65	1.15	0.64	0.89	99.52	9.02	11.6	855	29.9	130	168	54	79	8	20.4	73	28	663	—	—	-0.5	1.3	21	6	—	—	
21	H91-45	—	SE	SE	32	36	4	552070	4893260	Tmbas	BA	52.01	1.17	17.46	4.22	5.11	0.16	4.99	8.05	3.65	1.15	0.64	0.89	99.52	9.02	11.6	855	29.9	130	168	54	79	8	20.4	73	28	663	—	—	-0.5	1.3	21	6	—	—	
22	H91-47	—	SE	SE	32	36	4	553610	4893070	Tmbas	BTra	52.51	1.28	17.94	2.88	6.48	0.16	4.92	8.00	4.00	1.12	0.59	1.08	100.04	10.08	12	855	23	128	210	21	83	—	—	34	501	20	44	—	—	22	—	2.1	1.9	—	—
23	H91-47	—	SE	SE	32	36	4	553610	4893070	Tmbas	BTra	52.51	1.28	17.94	2.88	6.48	0.16	4.92	8.00	4.00	1.12	0.59	1.08	100.04	10.08	12	855	23	128	210	21	83	—	—	34	501	20	44	—	—	22	—	2.1	1.9	—	—
24	H91-47	—	SE	SE	32	36	4	553610	4893070	Tmbas	BTra	52.51	1.28	17.94	2.88	6.48	0.16	4.92	8.00	4.00	1.12	0.59	1.08	100.04	10.08	12	855	23	128	210	21	83	—	—	34	501	20	44	—	—	22	—	2.1	1.9	—	—
25	H91-47	—	SE	SE	32	36	4	553610	4893070	Tmbas	BTra	52.51	1.28	17.94	2.88	6.48	0.16	4.92	8.00	4.00	1.12	0.59	1.08	100.04	10.08	12	855	23	128	210	21	83	—	—	34	501	20	44	—	—	22	—	2.1	1.9	—	—
26	H91-47	—	SE	SE	32	36	4	553610	4893070	Tmbas	BTra	52.51	1.28	17.94	2.88	6.48	0.16	4.92	8.00	4.00	1.12	0.59	1.08	100.04	10.08	12	855	23	128	210	21	83	—	—	34	501	20	44	—	—	22	—	2.1	1.9	—	—
27	H91-47	—	SE	SE	32	36	4	553610	4893070	Tmbas	BTra	52.51	1.28	17.94	2.88	6.48	0.16	4.92	8.00	4.00	1.12	0.59	1.08	100.04	10.08	12	855	23	128	210	21	83	—	—	34	501	20	44	—	—	22	—	2.1	1.9	—	—
28	H91-47	—	SE	SE	32	36	4	553610	4893070	Tmbas	BTra	52.51	1.28	17.94	2.88	6.48	0.16	4.92	8.00	4.00	1.12	0.59	1.08	100.04	10.08	12	855	23	128	210	21	83	—	—	34	501	20	44	—	—	22	—	2.1	1.9	—	—
29	H91-47	—	SE	SE	32	36	4	553610	4893070	Tmbas	BTra	52.51	1.28	17.94	2.88	6.48	0.16	4.92	8.00	4.00	1.12	0.59	1.08	100.04	10.08	12	855	23	128																	

Preliminary Geologic Map of the Mount McLoughlin 7.5' Quadrangle, Jackson and Klamath Counties, Oregon

Table 1 (page 2).

Map no.	Sample no.	K-Ar Age ^a of 1/4 Ma	1/4 Sec. of 1/4	T. (°C)	R. (°E)	UTM m	Unit	Lith.	SiO ₂ (%)	TiO ₂ (%)	Al ₂ O ₃ (%)	Fe ₂ O ₃ (%)	FeO (%)	MnO (%)	MgO (%)	CaO (%)	Na ₂ O (%)	K ₂ O (%)	P ₂ O ₅ (%)	Total (%)	Fe ₂ O ₃ (%)	Rb (%)	Sr (%)	Y (%)	Zr (%)	V (%)	Ni (%)	Cr (%)	Nb (%)	Ga (%)	Cu (%)	Zn (%)	Co (%)	Ba (%)	La (%)	Ce (%)	U (%)	Th (%)	Sc (%)	Pb (%)	Yb (%)	Be (%)	
42	84-46	0.08 ± 0.03	SE	13	36	5	553470	Qbzm	55.62	1.03	17.21	1.33	5.41	0.13	4.75	7.43	3.84	1.17	0.38	0.45	100.09	7.94	7.8	852	155	50	179	17.6	26	2.4	22.5	99	59	22	224	7	14	1.4	3.5	20	4.7	0.8	1.1
43	84-38	<0.15	NE	14	36	4	553470	Qbzm	55.65	0.78	16.95	1.34	3.83	0.10	4.05	7.78	4.13	0.78	0.12	0.34	99.97	7.02	7.7	877	7.3	48	164	40	28	2.4	22.6	50	57	23	224	7	14	1.3	4.4	17	3.9	1	1
44	91-52	0.08 ± 0.03	NW	15	36	4	553480	Qbzm	56.27	0.78	16.96	1.34	4.05	0.10	4.02	7.78	4.13	0.78	0.12	0.34	99.97	7.02	7.7	895	14.4	45	162	28	45	2.5	22.3	19	56	22	234	8	19	1.3	4.4	17	3.9	1	1
45	91-49	0.05 ± 0.03	SE	15	36	4	553480	Qbzm	56.05	0.78	16.96	1.34	4.05	0.10	4.02	7.78	4.13	0.78	0.12	0.34	99.97	7.02	7.7	895	14.4	45	162	28	45	2.5	22.3	19	56	22	234	8	19	1.3	4.4	17	3.9	1	1
46	91-45	0.05 ± 0.03	SE	15	36	4	553480	Qbzm	56.05	0.78	16.96	1.34	4.05	0.10	4.02	7.78	4.13	0.78	0.12	0.34	99.97	7.02	7.7	895	14.4	45	162	28	45	2.5	22.3	19	56	22	234	8	19	1.3	4.4	17	3.9	1	1
47	M91-69	—	SE	15	36	4	553510	Qbzm	53.02	1.13	16.78	2.82	5.00	0.13	7.73	8.65	3.77	0.41	0.28	0.61	100.43	9.93	4	680	24	178	168	252	—	—	—	36	308	15	31	—	—	—	—	—	—	—	—
48	Q9SM-53A	—	NW	22	36	4	553510	Qbzm	53.02	1.13	16.78	2.82	5.00	0.13	7.73	8.65	3.77	0.41	0.28	0.61	100.43	9.93	4	680	24	178	168	252	—	—	—	36	308	15	31	—	—	—	—	—	—	—	—
49	M91-69	—	NW	22	36	4	553510	Qbzm	53.02	1.13	16.78	2.82	5.00	0.13	7.73	8.65	3.77	0.41	0.28	0.61	100.43	9.93	4	680	24	178	168	252	—	—	—	36	308	15	31	—	—	—	—	—	—	—	—
50	M91-69	—	NW	22	36	4	553510	Qbzm	53.02	1.13	16.78	2.82	5.00	0.13	7.73	8.65	3.77	0.41	0.28	0.61	100.43	9.93	4	680	24	178	168	252	—	—	—	36	308	15	31	—	—	—	—	—	—	—	—
51	Q9SM-52	—	NW	16	36	4	553440	Qbzm	54.41	0.77	16.95	1.33	5.41	0.13	4.75	7.43	3.84	1.17	0.38	0.45	100.09	7.94	7.8	852	155	50	179	17.6	26	2.4	22.5	99	59	22	224	7	14	1.4	3.5	20	4.7	0.8	1.1
52	Q9SM-53B	—	NW	16	36	4	553440	Qbzm	54.41	0.77	16.95	1.33	5.41	0.13	4.75	7.43	3.84	1.17	0.38	0.45	100.09	7.94	7.8	852	155	50	179	17.6	26	2.4	22.5	99	59	22	224	7	14	1.4	3.5	20	4.7	0.8	1.1
53	Q9SM-53B	—	NW	16	36	4	553440	Qbzm	54.41	0.77	16.95	1.33	5.41	0.13	4.75	7.43	3.84	1.17	0.38	0.45	100.09	7.94	7.8	852	155	50	179	17.6	26	2.4	22.5	99	59	22	224	7	14	1.4	3.5	20	4.7	0.8	1.1
54	M91-26	—	NW	16	36	4	553440	Qbzm	54.41	0.77	16.95	1.33	5.41	0.13	4.75	7.43	3.84	1.17	0.38	0.45	100.09	7.94	7.8	852	155	50	179	17.6	26	2.4	22.5	99	59	22	224	7	14	1.4	3.5	20	4.7	0.8	1.1
55	M91-26	—	NW	16	36	4	553440	Qbzm	54.41	0.77	16.95	1.33	5.41	0.13	4.75	7.43	3.84	1.17	0.38	0.45	100.09	7.94	7.8	852	155	50	179	17.6	26	2.4	22.5	99	59	22	224	7	14	1.4	3.5	20	4.7	0.8	1.1
56	84-41	—	NW	16	36	4	553440	Qbzm	54.41	0.77	16.95	1.33	5.41	0.13	4.75	7.43	3.84	1.17	0.38	0.45	100.09	7.94	7.8	852	155	50	179	17.6	26	2.4	22.5	99	59	22	224	7	14	1.4	3.5	20	4.7	0.8	1.1
57	M91-93	—	NW	16	36	4	553440	Qbzm	54.41	0.77	16.95	1.33	5.41	0.13	4.75	7.43	3.84	1.17	0.38	0.45	100.09	7.94	7.8	852	155	50	179	17.6	26	2.4	22.5	99	59	22	224	7	14	1.4	3.5	20	4.7	0.8	1.1
58	84-39	—	NW	16	36	4	553440	Qbzm	54.41	0.77	16.95	1.33	5.41	0.13	4.75	7.43	3.84	1.17	0.38	0.45	100.09	7.94	7.8	852	155	50	179	17.6	26	2.4	22.5	99	59	22	224	7	14	1.4	3.5	20	4.7	0.8	1.1
59	84-44	—	NW	16	36	4	553440	Qbzm	54.41	0.77	16.95	1.33	5.41	0.13	4.75	7.43	3.84	1.17	0.38	0.45	100.09	7.94	7.8	852	155	50	179	17.6	26	2.4	22.5	99	59	22	224	7	14	1.4	3.5	20	4.7	0.8	1.1
60	Q9SM-56	—	NW	16	36	4	553440	Qbzm	54.41	0.77	16.95	1.33	5.41	0.13	4.75	7.43	3.84	1.17	0.38	0.45	100.09	7.94	7.8	852	155	50	179	17.6	26	2.4	22.5	99	59	22	224	7	14	1.4	3.5	20	4.7	0.8	1.1
61	84-47	—	NW	16	36	4	553440	Qbzm	54.41	0.77	16.95	1.33	5.41	0.13	4.75	7.43	3.84	1.17	0.38	0.45	100.09	7.94	7.8	852	155	50	179	17.6	26	2.4	22.5	99	59	22	224	7	14	1.4	3.5	20	4.7	0.8	1.1
62	84-43	—	NW	16	36	4	553440	Qbzm	54.41	0.77	16.95	1.33	5.41	0.13	4.75	7.43	3.84	1.17	0.38	0.45	100.09	7.94	7.8	852	155	50	179	17.6	26	2.4	22.5	99	59	22	224	7	14	1.4	3.5	20	4.7	0.8	1.1
63	M91-82	—	NW	16	36	4	553440	Qbzm	54.41	0.77	16.95	1.33	5.41	0.13	4.75	7.43	3.84	1.17	0.38	0.45	100.09	7.94	7.8	852	155	50	179	17.6	26	2.4	22.5	99	59	22	224	7	14	1.4	3.5	20	4.7	0.8	1.1
64	84-45	—	NW	16	36	4	553440	Qbzm	54.41	0.77	16.95	1.33	5.41	0.13	4.75	7.43	3.84	1.17	0.38	0.45	100.09	7.94	7.8	852	155	50	179	17.6	26	2.4	22.5	99	59	22	224	7	14	1.4	3.5	20	4.7	0.8	1.1
65	84-42	—	NW	16	36	4	553440	Qbzm	54.41	0.77	16.95	1.33	5.41	0.13	4.75	7.43	3.84	1.17	0.38	0.45	100.09	7.94	7.8	852	155	50	179	17.6	26	2.4	22.5	99	59	22	224	7	14	1.4	3.5	20	4.7	0.8	1.1
66	84-46	—	NW	16	36	4	553440	Qbzm	54.41	0.77	16.95	1.33	5.41	0.13	4.75	7.43	3.84	1.17	0.38	0.45	100.09	7.94	7.8	852	155	50	179	17.6	26	2.4	22.5	99	59	22	224	7	14	1.4	3.5	20	4.7	0.8	1.1
67	Q9SM-7	—	NW	16	36	4	553440	Qbzm	54.41	0.77	16.95	1.33	5.41	0.13	4.75	7.43	3.84	1.17	0.38	0.45	100.09	7.94	7.8	852	155	50	179	17.6	26	2.4	22.5	99	59	22	224	7	14	1.4	3.5	20	4.7	0.8	1.1
68	Q9SM-7	—	NW	16	36	4	553440	Qbzm	54.41	0.77	16.95	1.33	5.41	0.13	4.75	7.43	3.84	1.17	0.38	0.45	100.09	7.94	7.8	852	155	50	179	17.6	26	2.4	22.5	99	59	22	224	7	14	1.4	3.5	20	4.7	0.8	1.1
69	84-40	—	NW	16	36	4	553440	Qbzm	54.41	0.77	16.95	1.33	5.41	0.13	4.75	7.43	3.84	1.17	0.38	0.45	100.09	7.94	7.8	852	155	50	179	17.6	26	2.4	22.5	99	59	22	224	7	14	1.4	3.5	20	4.7	0.8	1.1
70	M91-100	—	NW	16	36	4	553440	Qbzm	54.41	0.77	16.95	1.33	5.41	0.13	4.75	7.43	3.84	1.17	0.38	0.45	100.09	7.94	7.8	852	155	50	179	17.6	26	2.4	22.5	99	59	22	224	7	14	1.4	3.5	20	4.7	0.8	1.1
71	M91-96	—	NW	16	36	4	553440	Qbzm	54.41	0.77	16.95	1.33	5.41	0.13	4.75	7.43	3.84	1.17	0.38	0.45	100.09	7.94	7.8	852	155	50	179	17.6	26	2.4	22.5	99	59	22	224	7	14	1.4	3.5	20	4.7	0.8	1.1
72	M91-103C	—	NW	16	36	4	553440	Qbzm	54.41	0.77	16.95	1.33	5.41	0.13	4.75	7.43	3.84	1.17	0.38	0.45	100.09	7.94	7.8	852	155	50	179	17.6	26	2.4	22.5	99	59	22	224	7	14	1.4	3.5	20	4.7	0.8	1.1
73	M91-20	—	NW	16	36	4	553440	Qbzm	54.41	0.77	16.95	1.33	5.41	0.13	4.75	7.43	3.84	1.17	0.38	0.45	100.09	7.94	7.8	852	155	50	179	17.6	26	2.4	22.5	99	59	22	224	7	14	1.4	3.5	20	4.7	0.8	1.1
74	M91-69	—	NW	16	36	4	553440	Qbzm	54.41	0.77	16.95	1.33	5.41	0.13	4.75	7.43	3.84	1.17	0.38	0.45	100.09	7.94	7.8	852	155	50	179																